ISSN 1580-4003

THE SCIENTIFIC JOURNAL OF THE VETERINARY FACULTY UNIVERSITY OF LJUBLJANA

SLOVENIAN VETERINARY RESEARCH

SLOVENSKI VETERINARSKI ZBORNIK

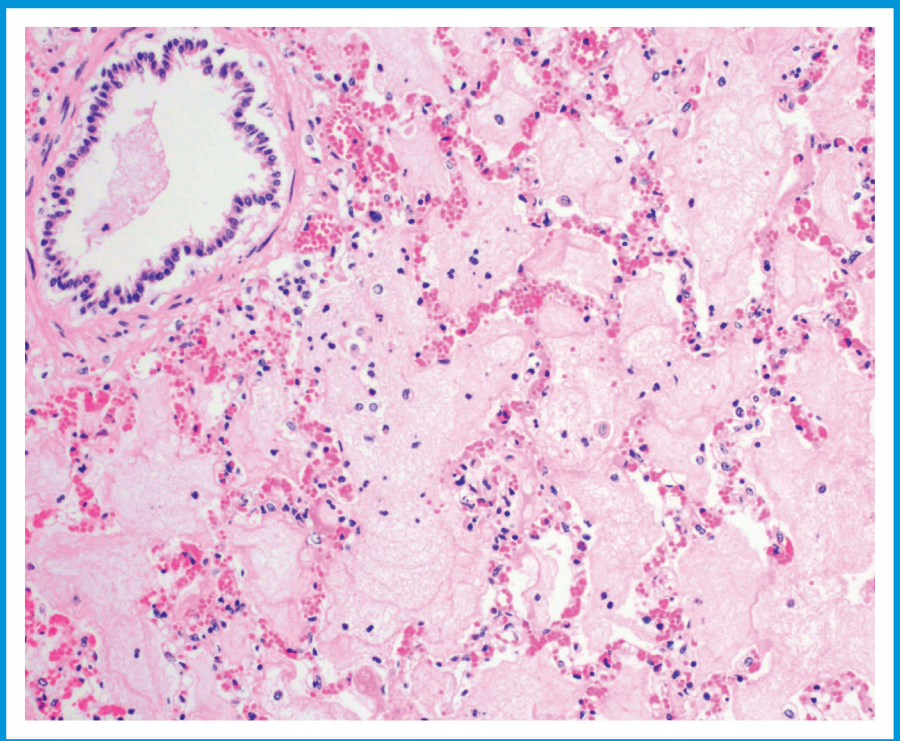

Slov Vet Res 2015; 52 (2): 45-102

Volume 52 2

Slov Vet Res • Ljubljana • 2015 • Volume 52 • Number 2 • 45-102

THE SCIENTIFIC JOURNAL OF THE VETERINARY FACULTY UNIVERSITY OF LJUBLJANA

SLOVENIAN VETERINARY RESEARCH

SLOVENSKI VETERINARSKI ZBORNIK

Volume 52 2

Slov Vet Res • Ljubljana • 2015 • Volume 52 • Number 2 • 45-102

The Scientific Journal of the Veterinary Faculty University of Ljubljana

SLOVENIAN VETERINARY RESEARCH
SLOVENSKI VETERINARSKI ZBORNIK

Previously: RESEARCH REPORTS OF THE VETERINARY FACULTY UNIVERSITY OF LJUBLJANA
Prej: ZBORNIK VETERINARSKE FAKULTETE UNIVERZA V LJUBLJANI

4 issues per year / izhaja štirikrat letno

Address: Veterinary Faculty, Gerbičeva 60, 1000 Ljubljana, Slovenia
Naslov: Veterinarska fakulteta, Gerbičeva 60, 1000 Ljubljana, Slovenija
Tel.: +386 (0)1 47 79 100, 47 79 129, Fax: +386 (0)1 28 32 243
E-mail: slovetres@vf.uni-lj.si

Sponsored by the Slovenian Book Agency
Sofinancira: Javna agencija za knjigo Republike Slovenije

ISSN 1580-4003
Printed by / tisk: DZS, d.d., Ljubljana
Indexed in / indeksirano v: Agris, Biomedicina Slovenica, CAB Abstracts, IVSI
Urlich's International Periodicals Directory, Science Citation Index Expanded,
Journal Citation Reports/Science Edition
http://www.slovetres.si/

SLOVENIAN VETERINARY RESEARCH
SLOVENSKI VETERINARSKI ZBORNIK

Slov Vet Res 2015; 52 (2)

Original Scientific Articles

Špehar M, Mrak V, Smetko A, Potočnik K, Gorjanc G. Genome-wide association study for dairy traits in Slovenian Brown Swiss breed 49
Jaćimović M, Lenhardt M, Višnjić-Jeftić Ž, Jarić I, Gačić Z, Hegediš A, Krpo-Ćetković J. Elemental concentrations in different tissues of European perch and black bullhead from Sava Lake (Serbia) 57
Smodiš Škerl MI, Gregorc A. Characteristics of hypopharyngeal glands in honeybees (*Apis mellifera carnica*) from a nurse colony 67
Krek JL, Šimundić M, Drab M, Pajnič M, Šuštar V, Štukelj R, Drobne D, Veronika Kralj-Iglič V. Effect of carbon black nanomaterial on canine erythrocyte and platelet shape 75
Bogićević S, Živin M. Efficacy of potential atypical antipsychotic lek-8829 on behavioral effects in rat model of catalepsy and inhibition of amphetamine induced psychomotor stimulation..... 87

Case Report

Burgstaller J, Sick K, Mansfeld MD, Steinparzer R, Wittek T. Peracute alpha-naphthylthiourea intoxication in a cow-calf herd ... 97

Slov Vet Res 2015; 52 (2): 49-55
UDC 636.2.082.2:575.11/21

Original Scientific Article

GENOME-WIDE ASSOCIATION STUDY FOR DAIRY TRAITS IN SLOVENIAN BROWN SWISS BREED

Marija Špehar[1,2*], Vesna Mrak[2], Anamarija Smetko[1], Klemen Potočnik[2], Gregor Gorjanc[2,3]

[1]Croatian Agricultural Agency, Ilica 101, 10000 Zagreb, Croatia; [2]Department of Animal Science, Biotechnical Faculty, University of Ljubljana, Groblje 3, 1230 Domžale, Slovenia; [3]The Roslin Institute and Royal (Dick) School of Veterinary Studies, The University of Edinburgh, Easter Bush, Midlothian, EH25 9RG, Scotland, UK

*Corresponding author, E-mail: mspehar@hpa.hr

Summary: Genome-wide association studies (GWAS) based on thousands of single nucleotide polymorphisms (SNPs) allows exploring genes associated with economically important traits. The objective of this study was to perform GWAS in small population of genotyped bulls of Slovenian Brown Swiss (BSW) breed to identify SNP markers associated with dairy traits: milk yield (MY), fat yield (FY), and protein yield (PY). The daughter yield deviations of 182 progeny tested bulls were used as phenotypes. For each bull, genotypes were scored for 34,450 SNPs across the whole genome. Single SNP analysis was performed to detect significant associations among SNPs and dairy traits across the genome. Two models were considered: 1) linear regression model considering one marker at a time, and 2) linear regression model with admixture components for accounting population stratification. The Bonferroni correction resulted in 52 significant SNPs using model 1). Correction for population stratification based on selected criteria was shown to have great impact on the analysis and then no significant associations among SNPs and dairy traits have been detected. Therefore, the results were sensitive to population stratification and together with the small data set did not give much power to accurately estimate associations. Further improvements should be made on the enlargement of number of genotyped bulls in order to detect association signals and the identification of genes associated with dairy traits in Slovenian BSW breed.

Key words: GWAS; dairy traits; single SNP analysis; population stratification

Introduction

In the dairy cattle production, all economically important traits are influenced by many genes that appear as continuous variation (1). The inclusion of molecular information i.e. thousands of single nucleotide polymorphisms (SNPs) in selection schemes made the use of this information in selection decisions feasible, through a technique commonly called genomic selection (2). Genomic selection improves the level of genetic gain, compared to traditional selection based on progeny test, increased accuracy of EBV of young or non-phenotyped animals from about 0.60 (parent average) to 0.80 (3). Even though these accuracies are lower than with progeny test the early use of young bulls shortens generation interval considerably and therefore increases genetic gain per unit of time (4). Development of SNP marker panels also enabled genome wide association studies (GWAS) with a purpose to determine associations between DNA polymorphisms and phenotypes of interest and to identify chromosome regions that harbour genes

Received: 24 June 2014
Accepted for publication: 4 February 2015

or regulatory elements related to traits (5). GWAS has been implemented in livestock species, such as cattle, to discover superior variants of all genes contributing to the phenotype of economically important dairy (6, 7, 8), meat (9), and health traits (10). Genomic selection and GWAS can be successfully implemented due to existing linkage disequilibrium (LD) between markers and QTL for the trait of interest (3).

The Brown Swiss (BSW) breed is a cosmopolitan breed selected for dairy characteristics and ability to produce in less favoured areas mostly in Alpine regions of Austria, Germany, Italy, Switzerland, and Slovenia. Original Brown breed (Braunvieh) from Switzerland was exported to the United States in 1869 (11), and after strong selection of this breed, previously classified as a dual-purpose breed, it was established as a dairy type and received a name Brown Swiss breed. Development of Slovenian BSW breed started at the beginning of 20th century when Original Brown breed bulls were imported from Austria and Switzerland with the manner to improve cows of local grey cattle. Lately also breeding heifers were imported. From the 1960s, the American BSW breeding bulls were used for improving cows of Brown breed in order to increase milk production (12). Bulls with 50% of American BSW genotype were imported from neighbouring countries. Moreover, five bulls with 100% American BSW genotype were also used for insemination. From 1976 to 1980 bulls were no longer imported but have been bred in Slovenia. The breed is mainly spread in the western part of Alpine area, as well as southern and northern part of Slovenia with harsh environmental conditions. According to the annual report (13), 6.95% of all active cattle (or 31,087 heads) belong to the BSW breed. It is the second most important breed for milk production (13). The average production is 5,554 kg of milk in the standard lactation with 4.06% of fat and 3.39% of protein content.

In dairy cattle, and BSW breed too, the population stratification may exist. It could be result of selection that caused allele frequency changes (14) and artificial insemination which increased the presence of related animals in a randomly selected samples and the presence of large half-sib families (15). A potential challenge in GWAS is the presence of population stratification (family substructure) that can result in false-positive or negative associations and may lead to confounding results (16, 17). In order to take into account population stratification linear models have been suggested as a method of choice to reduce effect of false-positive or negative associations (18).

In this study, we conducted genome-wide association analysis of dairy traits: milk yield (MY), fat yield (FY), and protein yield (PY) in a small population of genotyped bulls of Slovenian BSW breed. We used the Illumina Bovine SNP50 Bead Chip to identify SNPs associated with dairy traits without and considering population stratification.

Material and methods

Phenotypes used were daughter yield deviations (DYDs) of dairy traits (MY, FY, and PY) taken from the routine national genetic evaluation. Altogether, DYDs for 182 progeny tested and genotyped BSW bulls born between 1990 and 2007 were included in the analysis. Bulls used in analysis predominantly originated from Slovenia. The exceptions were nine bulls imported to Slovenia as live animals from Austria and Germany. These bulls were used only in Slovenia. The DNA was extracted from semen samples and genotyped using the Illumina Bovine SNP50 Bead Chip (Illumina, San Diego, CA). Several quality controls were applied to the genotype data to investigate the integrity and informativeness of SNPs. These controls included genotyping call rate (CR) by SNP and by animal, minor allele frequency (MAF), departure from Hardy–Weinberg equilibrium (HWE) and parent–progeny conflicts (PPC). Data editing was carried out using SAS package (19). Number of SNPs excluded from the analysis differed among filtering criteria. SNPs were included in the analysis if CR was higher than 90% by the SNP. Altogether, 5,975 SNPs failed this criterion and were excluded from the analysis. SNPs with MAF lower than 0.05 (10,619 cases) were also excluded. The departure from HWE with a threshold of $P<10^{-5}$ excluded 538 SNPs from data set. The mean of PPC was low (<0.0001%) and below the threshold (<200 discrepancies) set for the data exclusion. SNPs that could not be mapped in BTA (1,672) or SNPs placed on X chromosome (747) were also excluded from the analysis. The final genotype file included 34,450 SNPs placed on 29 *Bos Taurus* autosomes (BTA) for 182 BSW bulls. Missing genotypes were imputed using the gpig program (20) based on method that approximates the gene content (21). Two types of analyses were conducted to detect SNP association signals.

Initially, a single trait GWAS was used to estimate genome-wide associations between phenotypes and SNPs for each of dairy traits. GWAS between phenotypes and SNP markers for each dairy trait were estimated using the following univariate linear mixed model to estimate association for one marker at a time:

$$\boldsymbol{y} = \boldsymbol{X}\boldsymbol{b} + \boldsymbol{e} \quad (1)$$

where $\boldsymbol{y}$ is a vector of phenotype values (DYDs), $\boldsymbol{b}$ is a vector that holds the intercept and allele substitution effect for the SNP marker of interest, while $\boldsymbol{X}$ is the incidence matrix linking $\boldsymbol{y}$ respectively with $\boldsymbol{b}$, and $\boldsymbol{e} \sim N(\boldsymbol{0}, \boldsymbol{I}\sigma_e^2)$ is a vector of residuals. Then, admixture components adjusting for population stratification were included in the model as covariates.

Admixture analysis was performed on the data using Admixture software (22) to determine the proportion of genotypes originated from different clusters in the population (K). The proportion of each subpopulation was estimated as unsupervised analysis assuming from two to ten populations. Finally, bulls were divided in four clusters coming from different ancestral populations. Separation was determined using admixture cross-validation procedure, which gives standard error of the cross validation estimate. R software package (23) was used to test associations between SNPs and dairy traits. Significance threshold was calculated using the Bonferroni correction for multiple testing. Estimated effects were transformed to negative logarithm of *p-values* of significant effects. Correction based on *p-value* (0.05) resulted in a Bonferroni threshold of 1.45×10^{-6}. SNPs with –log *(p-values)* above the Bonferroni threshold were considered significant.

Results

The distribution of observed distributions of –log (*p-value)* for each SNP was compared to the expected distribution under no-association (red line) in a quantile-quantile (Q-Q) plot for each dairy trait (Figure 1). Q-Q plot of data without accounting population stratification (black line) for all analysed traits showed an early separation of the observed and expected distribution (red line) indicating that the model which neglected family relationship was problematic. The fact that the black dots are above the diagonal axis on a Q-Q plot shows an elevated amount of statistical

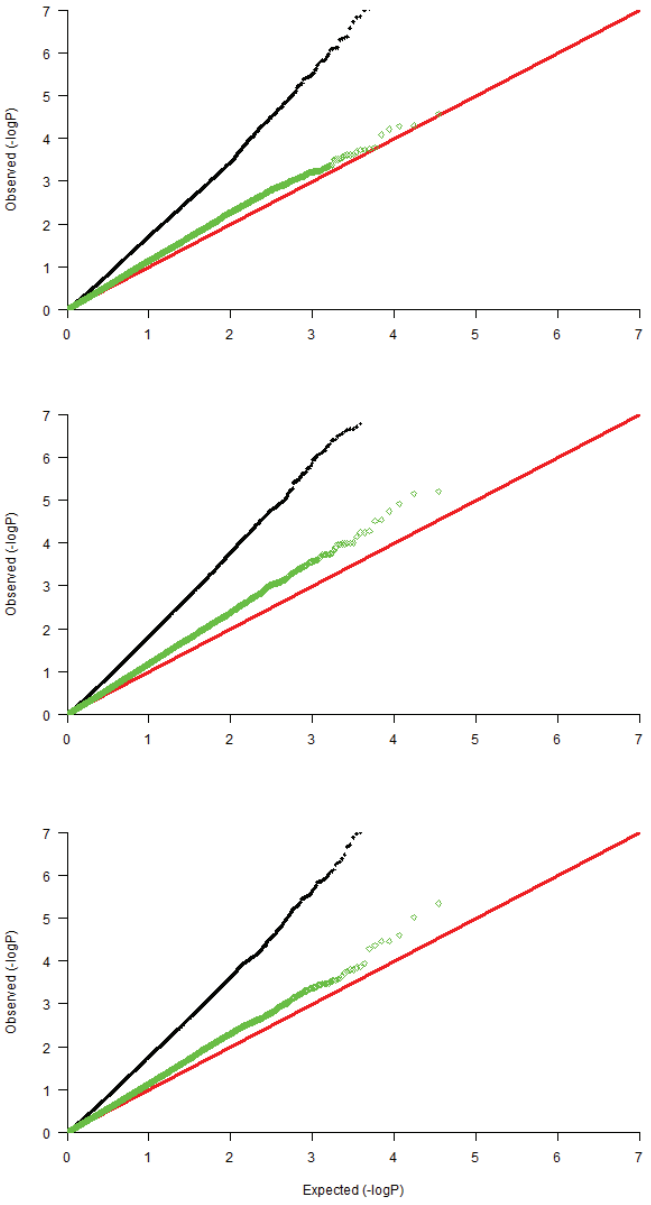

Figure 1: Q-Q plot for MY, FY, and PY. Red line is expected distribution, black dots are GWAS estimates without stratification, and green dots are GWAS estimates with stratification added to analysis

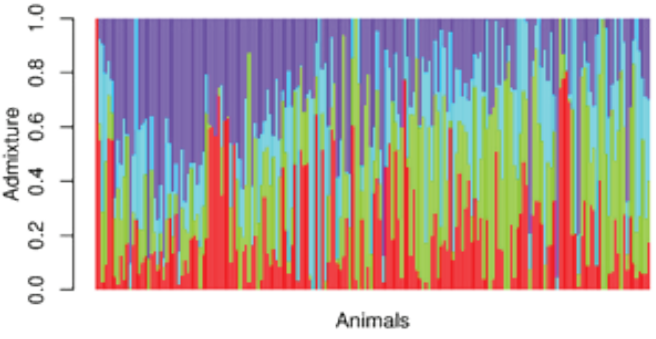

Figure 2: The proportion of subpopulations in each BSW bull estimated by Admixture analysis

significance for a huge number of variants, which is probably the result of population stratification. After correction, the data were well-behaved (green line) however for the majority of SNPs there was no more statistical significance.

For inclusion of population stratification components to the model, four ancestral populations were accepted as the best match describing population stratification due to lowest cross-validation error in K=4. Different genotype proportions per animal divided population in four clusters (Figure 2) which were added as a fixed effect, affecting SNP influence in GWAS analysis.

In total, 52 SNPs with a significant effect on MY, FY, and PY were identified by single trait analysis without considering population stratification. Among these, 11 were significant for all dairy traits. The associations were spread over 14 chromosomes. The majority of SNPs associated with MY were placed on the BTA21 followed by BTA9. The majority of genome-wide significant SNPs for FY and PY were also located on BTA 21 and BTA9. Manhattan plots based on the negative logarithm of *p-value* (y axis) of each SNP versus its chromosomal locations (x axis) for MY, FY; and PY are shown in Figure 3. Horizontal dashed line indicates the Bonferroni-corrected significance level.

Correction for population stratification based on the selected criteria was shown to have large impact on the results of analysis. No significant associations between SNPs and dairy traits have been detected (Figure 3 - right side).

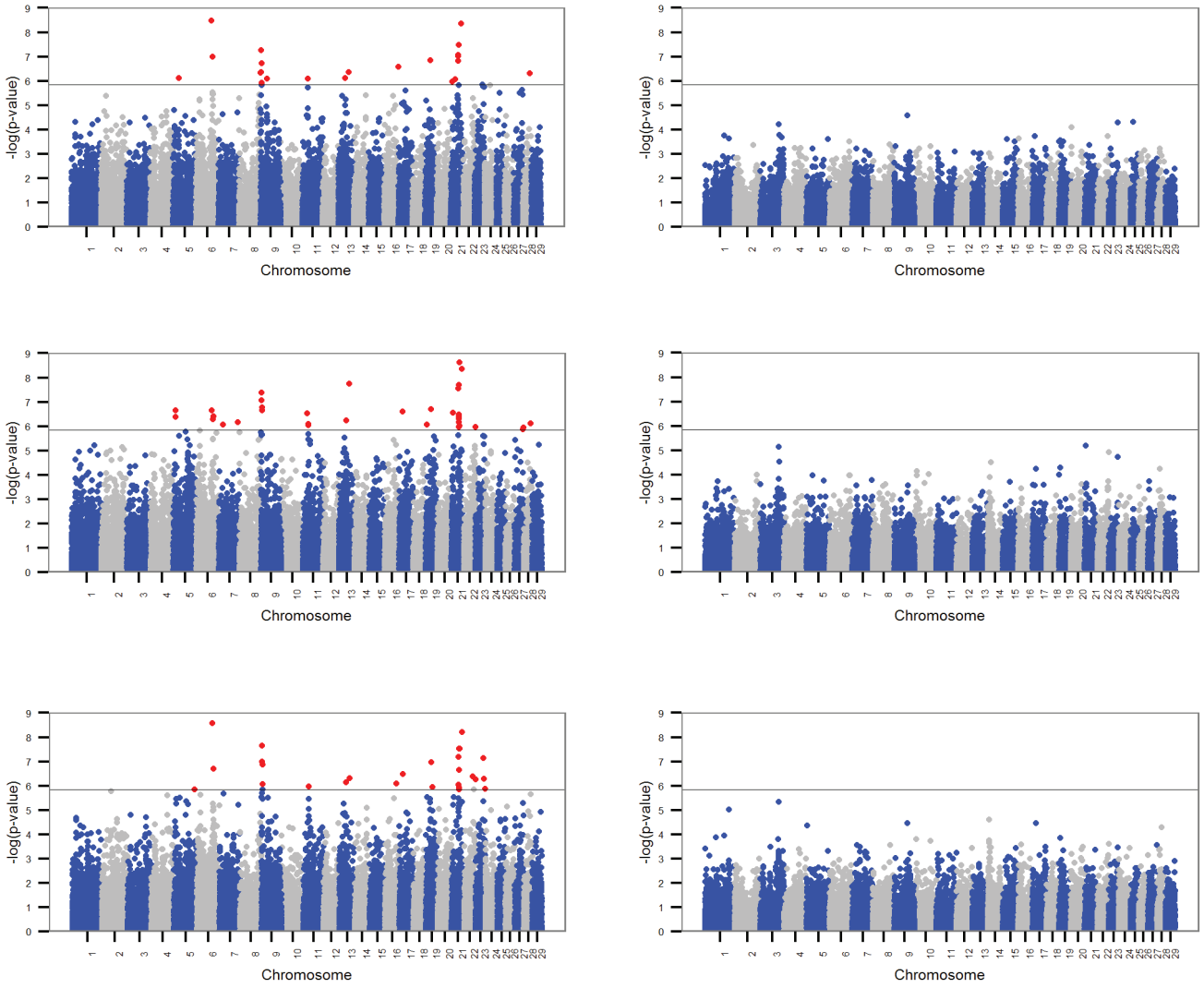

Figure 3: Manhattan plots for MY, FY, and PY using single SNP analysis without (left side) and with (right side) population stratification

Discussion

Single trait genome-wide analysis for dairy traits was presented to address the aspects of the GWAS for implementation of genomic selection in Slovenian BSW breed. The approach was used to estimate genome-wide associations between phenotypes and SNP markers based on data from national genetic evaluation. The effect of population stratification was taken into account since it was known from earlier publications (24, 26) that BSW breed is dealing with population stratification which has an impact on the results of GWAS. In the mentioned studies, principal component analysis was used to adjust the effect of population stratification. For studied population, animals were divided from two to ten ancestral clusters and according to the lowest cross validation error it was decided to take four clusters as best representation of stratification. After correction for population stratification, the data fitted more closely to the expected distribution on Q-Q plot (see Figure 1, green line) but then there were no statistically significant SNPs for investigated traits. Therefore, the results were sensitive to population stratification and together with the small sample size did not give much power to accurately estimate associations. Sample size must be increased by a factor of $1/r^2$ (where r^2 is a measure of linkage disequilibrium between pairs of biallelic markers) to detect an ungenotyped QTL, compared with the sample size for testing the QTL itself (25). Similar study but with higher number of bulls (554) of German Braunvieh (26) found five SNPs with the significant effect on dairy traits. Two SNPs which affected MY were placed on the BTA4, two SNPs associated FY were on the BTA14 and BTA23, while significant SNP with an effect on the fat content was on the BTA1. The largest data set (7,038 bulls) considering BSW breed (24) was based on large scale data from the international genetic evaluation. The total number of significant SNPs was 16 that affected dairy traits, with the strongest signal on the BTA25 (24). SNP associations for MY and PY were located on the same chromosome like in studies of Finnish Ayrshire (27) and Holstein (28) breed. GWAS in the dairy cattle mainly focused on the Holstein breed due to worldwide spreading (7). For MY, significant SNPs were located on BTA8, BTA9, BTA10, BTA11, BTA13, BTA25, and BTA29 (6, 8, 29). BTA14 has also been in focus since many studies reported DGAT1 as a major gene affecting milk traits (8, 29, 30). In this study, the association between SNPs and dairy traits was not detected in the DGAT1 region.

Conclusion

In the present study, the preliminary results from GWAS analysis were reported for dairy traits based on the small population of genotyped bulls of Slovenian BSW breed. Altogether, 52 SNPs with a significant effect on MY, FY, and PY were identified using single SNP analysis. After adjusting for population stratification, no significant associations between SNPs and dairy traits have been detected. Based on the analysis that considered afore mentioned criteria we could conclude that population stratification exists in the analysed data set and the model without adjustment was not dealing properly with the stratification in the data. Further improvements should be made on the enlargement of the number of genotyped bulls in order to detect association signals and the identification of genes associated with dairy traits. Results from GWAS will facilitate the understanding of the genetic architecture of complex traits.

References

1. Falconer DS, Mackay TFC. Introduction to quantitative gnetics. 4th ed. Harlow; Essex: Longman Green, 1996: 98–20.

2. Meuwissen THE, Hayes BH, Goddard ME. Prediction of total genetic value using genome-wide dense marker maps. Genetics 2001; 157: 1819–29.

3. Hayes BJ, Bowman PJ, Chamberlain AJ, Goddard ME. Invited review: Genomic selection in dairy cattle: progress and challenges. J Dairy Sci 2009; 92: 433–43.

4. Schaeffer LR. Strategy for applying genome-wide selection in dairy cattle. J Anim Breed Genet 2006; 123: 218–23.

5. Goddard ME, Hayes BJ. Mapping genes for complex traits in domestic animals and their use in breeding programmes. Nat Rev Genet 2009; 10: 381–391.

6. Bolormaa S, Pryce JE, Hayes BJ, Goddard ME. Multivariate analysis of a genome-wide asso-

ciation study in dairy cattle. J Dairy Sci 2010; 93: 3818–33.

7. Pryce JE, Bolormaa S, Chamberlain AJ, et al. A validated genome-wide association study in 2 dairy cattle breeds for milk production and fertility traits using variable length haplotypes. J Dairy Sci 2010; 93: 3331–45.

8. Mai MD, Sahana G, Christiansen FB, Guldbrandtsen B. A genome-wide association study for milk production traits in Danish Jersey cattle using a 50K single nucleotide polymorphism chip. J Anim Sci 2010; 88: 3522–8.

9. Bolormaa S, Porto Neto LR, Zhang YD, et al. A genome-wide association study of meat and carcass traits in Australian cattle. J Anim Sci 2011; 89: 2297–309.

10. Murdoch BM, Murdoch GK, Settles M, McKay S, Williams JL, Moore SS. Genome-wide scan identifies loci associated with classical BSE occurrence. PLoS ONE 2011; 6(11): e26819 (7 p.) http://www.plosone.org/article/fetchObject.action?uri=info:doi/10.1371/journal.pone.0026819&representation=PDF (10. Oct. 2014)

11. Yoder DM, Lush JL. A genetic history of the Brown Swiss cattle in the United States. J Hered 1937; 28: 154–60.

12. Ferčej J, Pogačar J, Lovšin N, Nendl B. Oplemenjevanje rjave pasme z ameriško rjavo. Sodob Kmet 1980; 4: 136–9.

13. Sadar M, Jenko J, Jeretina J, et al. Rezultati kontrole prireje mleka in mesa 2013. Ljubljana: Kmetijski inštitut Slovenije, 2014: 89 str. http://www.govedo.si/files /cpzgss/knjiznica/porocila/kontrola_porocila/REZULTATI_KONTROLE_2013.pdf (28. Oct. 2014)

14. Devlin B, Roeder K. Genomic control for association studies. Biometrics 1999; 55: 997–1004.

15. Ma L, Wiggans GR, Wang S, et al. Effect of sample stratification on dairy GWAS results. BMC Genomics 2012; 13: e536 (18 p.)
http://www.biomedcentral.com/content/pdf/1471-2164-13-536.pdf (16. Oct. 2014)

16. Kang HM, Zaitlen NA, Wade CM, et al. Efficient control for population structure in model organism association mapping. Genetics 2008; 178:1709–23.

17. Pritchard JK, Stephens M, Rosenberg N, Donnelly P. Association mapping in structured populations. Am J Hum Genet 2000; 67: 170–81.

18. Sonstegard TS, Ma L, Van Tassell CP, et al. Forty years of artificial selection in U.S. Holstein cattle had genome-wide signatures. In: 9th World Congress on Genetics Applied to Livestock Production: poster presentation. Leipzig, 2010.
https://www.aipl.arsusda.gov/publish/presentations/WC9_10/WC9_10_yang_da.pdf (28. Oct. 2014)

19. SAS Institute. SAS/STAT Software, Version 9.3. Cary, NC, 2011.

20. Strandén I. Manual for gpig program: pedigree based imputation of genotypes. Jokioinen, Finland : Biotechnology and Food Research, Biometrical Genetics, MTT Agrifood Research Finland, 2010: 13 p.

21. Gengler N, Mayeres P, Szydlowski M. A simple method to approximate gene content in large pedigree populations: application to the myostatin gene in dual-purpose Belgian Blue cattle. Animal 2007; 1: 21–8.

22. Alexander DH, Novembre J, Lange K. Fast model-based estimation of ancestry in unrelated individuals. Genome Res 2009; 19: 1655–64.

23. R Development Core Team. R: a language and environment for statistical computing. R Foundation for Statistical Computing. Vienna, Austria, 2011 ISBN 3-900051-07-0. http://www.R-project.org (28 Oct. 2014).

24. Guo J, Jorjani H, Carlborg O. A genome-wide association study using international breeding-evaluation data identifies major loci affecting production traits and stature in the Brown Swiss cattle breed. BMC Genet 2012; 13: 82–92.

25. Pritchard JK, Przeworski M. Linkage disequilibrium in humans: models and data. Am J Hum Genet 2001; 69: 1–14.

26. Maxa J, Neuditschko M, Russ I, Förster M, Medugorac I. Genome-wide association mapping of milk production traits in Braunvieh cattle. J Dairy Sci 2012; 95: 5357–64.

27. Viitala SM, Schulman NF, Koning DJ, et al. Quantitative trait loci affecting milk production traits in Finnish Ayrshire dairy cattle. J Dairy Sci 2003; 86: 1828–36.

28. Harder B, Bennewitz J, Reinsch N, et al. Mapping of quantitative trait loci for lactation persistency traits in German Holstein dairy cattle. J Anim Breed Genet 2006; 123: 89–96.

29. Jiang L, Liu J, Sun D, et al. Genome wide association studies for milk production traits in Chinese Holstein population. PLoS ONE 2010; 5(10): e13661 (12 p.) http://www.plosone.org/article/fetchObject.action?uri=info:doi/10.1371/journal.pone.0013661&representation=PDF (28.

Oct. 2014)

30. Grisart B, Coppieters W, Farnir F, et al. Positional candidate cloning of a QTL in dairy cattle: identification of a missense mutation in the bovine DGAT1 gene with major effect on milk yield and composition. Genome Res 2002; 12: 222–31.

ASOCIACIJSKE ŠTUDIJE NA CELOTNEM GENOMU ZA LASTNOSTI MLEČNOSTI PRI SLOVENSKI RJAVI PASMI

M. Špehar, V. Mrak, A. Smetko, K. Potočnik, G. Gorjanc

Povzetek: Asociacijske študije na celotnem genomu (GWAS), ki temeljijo na več tisoč polimorfizmih na posameznih nukleotidih (SNP), nam omogočajo, da lahko najdemo gene povezane z gospodarsko pomembnimi lastnostmi. Cilj raziskave je bil narediti GWAS z namenom identifikacije označevalcev SNP, ki so povezani z lastnostmi mlečnosti: količina mleka (MY), količina maščob (FY) in količina beljakovin (PY) v majhni populaciji genotipiziranih bikov slovenske rjave pasme. Kot fenotipske meritve smo uporabili odstopanja hčera 182 progeno testiranih bikov. Genotip za vsakega bika je bil poznan na 34,450 označevalcih SNP porazdeljenih po celem genomu. V študiji je bila narejena analiza polimorfizmov na posameznem označevalcu za odkrivanje označevalcev SNP, povezanih z lastnostmi mlečnosti na celotnem genomu. Uporabljena sta bila dva modela: 1) linearni regresijski model ob upoštevanju enega označevalca naenkrat in 2) komponente admiksture analize, ki so bile vključene v prvi model, da se je upoštevala razdeljenost populacije. Bonferroni korekcija je pokazala 52 statistično značilnih označevalcev SNP, ki so temeljili na modelu 1). Korekcija na razdeljenost populacije na podpopulacije na podlagi izbranih kriterijev se je pokazala kot ključna. Z uporabo modela 2) nismo odkrili značilnih povezav med označevalci SNP in lastnostmi mlečnosti. Zaradi tega so bili rezultati občutljivi na razdeljenost populacije na podpopulacije in skupaj z majhnim številom podatkov niso veliko pripomogli k bolj natančni oceni povezav. Nadaljnje izboljšave bi lahko naredili s povečanjem števila genotipiziranih bikov, z namenom, da bi odkrili povezane signale in identificirali gene, povezane z lastnostmi mlečnosti pri slovenski rjavi pasmi.

Ključne besede: GWAS; lastnosti mlečnosti; analiza polimorfizmov na posameznem nukleotidu; razdeljenost populacije

Slov Vet Res 2015; 52 (2): 57-65
UDC 502.51:504.5:546.3:597.551.41:597.556.33(497.11)

Original Scientific Article

ELEMENTAL CONCENTRATIONS IN DIFFERENT TISSUES OF EUROPEAN PERCH AND BLACK BULLHEAD FROM SAVA LAKE (SERBIA)

Milica Jaćimović[1], Mirjana Lenhardt[2], Željka Višnjić-Jeftić[1], Ivan Jarić[1*], Zoran Gačić[1], Aleksandar Hegediš[1,3], Jasmina Krpo-Ćetković[3]

[1]Institute for Multidisciplinary Research, University of Belgrade, Kneza Višeslava 1, 11030 Belgrade, [2]Institute for Biological Research "Siniša Stanković", University of Belgrade, Bulevar Despota Stefana 142, 11060 Belgrade, [3]Faculty of Biology, University of Belgrade, Studentski trg 16, 11000 Belgrade, Serbia

*Corresponding author, E-mail: ijaric@imsi.bg.ac.rs

Summary: Distribution of 17 chemical elements in gills, muscle, and liver of the European perch (*Perca fluviatilis*) and black bullhead (*Ameiurus melas*) from the Sava Lake (Serbia) was studied to detect bioaccumulation patterns in relation to the species' diet and trophic level. Concentrations of Ba, Cd, Co, Cr, Li, Ni, Pb, B, and Se were below the detection limits. Concentrations of Al, Fe, Mn, Sr, and Zn were higher in gills of the black bullhead; As, Mo, and Sr were higher in liver of the European perch; Fe and Zn were higher in liver of the black bullhead. In muscle, a significant difference between species was found only for Sr. Copper was detected only in liver of the black bullhead. Similarity in elemental concentrations in both species could be explained by a relatively similar diet of these two species, while the differences, especially in gills, could be explained by different habitat preferences.

Key words: heavy metal; pollution; Percidae; Ictaluridae; Danube River

Introduction

In recent years, one of the environmental problems of increasing concern is the contamination of freshwater fish with metals, which enter the water bodies through atmosphere, drainage, surface runoff, and soil erosion (1). While some metals are required as essential nutrients for fish, including copper, selenium, iron and zinc, their over-accumulation can pose a food safety concern. For this reason, Food and Agriculture Organization (2) declared that metals or chemicals of particular concern include arsenic, cadmium, chromium, lead, methyl mercury, nickel and selenium. Iron is not toxic to fish, but long-term exposure to high levels can be harmful (3). Iron is present in proteins such as haemoglobin and myoglobin and stored in proteins such as ferritin and hemosiderin, which are found in high concentrations in the fish liver (4). According to (5), molybdenum is relatively non-toxic to fish as compared to other metals,

Received: 25 July 2014
Accepted for publication: 2 February 2015

and exposure to sub-lethal concentrations of molybdenum activates neither physiological nor cellular stress response in fish.

Metals enter the fish body through the body surface, gills, or digestive tract (6) causing numerous physiological disorders. The toxic effects of metals may cause inner organ alterations, immune system disturbances, changes in blood parameters, and the reduction of organism's overall vitality and resistance to diseases, influencing individual growth rates, reproduction and mortality (7). Metals can also lead to increased mortality of fish fry and loss of genetic variability (1). Heavy metal contamination of freshwater fish represents a problem not only for piscivorous fish, birds, and mammals that consume contaminated prey (8), but also a potential human health associated with fish consumption (9).

According to (8), metal uptake and accumulation in fish is a complex process that depends on metal concentration, time of exposure, source of metal uptake, environmental conditions (water temperature, pH, hardness, salinity), and intrinsic factors (fish age, feeding habits). Various metals also differ in their affinity for different fish tissues (10). As their concentrations tend to increase along the food chain through biomagnification, piscivorous fish are often able to accumulate higher metal concentrations (10).

Feeding habits, behaviour, and regulatory ability can influence the accumulation patterns of a species (11). European perch (*Perca fluviatilis* L.) and black bullhead (*Ameiurus melas* Rafinesque) have the capacity to tolerate general disturbances in the environment. Both species are opportunistic and piscivorous when they reach adult age, with the difference that European perch is a diurnal feeder, while black bullhead is restricted to nocturnal feeding, as all ictalurids (12). Both species exhibit ontogenetic diet shifts: juvenile European perch feeds on zooplankton, subadults feed on benthic macroinvertebrates, and adults feed on fish (13); juvenile black bullhead feeds mainly on larvae/nymphs of aquatic insects, leeches, and crustaceans, while adults also feed on clams, snails, plant material, and fishes (14).

Gills, muscle, and liver are considered to be three key tissues in the monitoring of heavy metal accumulation in fish (15). Gills represent the primary site of metal uptake from the water. Although muscle tissue has a low metal accumulating ability, it is essential to include it in monitoring programs due to its role in the human diet (16). Liver is the organ with detoxificating and accumulating role (3), and appears to be the main heavy metal storage tissue (17).

In the present study we investigate the distribution and accumulation of 17 metals and trace elements in gills, muscle, and liver of the European perch and black bullhead in the Sava Lake, Serbia. The aim of the study was to detect the bioaccumulation patterns in the selected species in relation to their diet and trophic level. The study is also important from the human health perspective, because the Sava Lake represents an important recreational area, with more than 150.000 visitors per day during the high season, and concentrations of metals and trace elements accumulated in fish tissues are good indicators of water contamination and pollution. Moreover, these two fish species are used for human consumption.

Material and methods

Study area

This study was conducted in Sava Lake (44°47'17.08'' N, 20° 24' 35.75'' E), formerly a right-hand branch of the Sava River, located next to the river island Ada Ciganlija (Fig. 1). This 86 ha lake is located in the city of Belgrade, within the urban area (18).

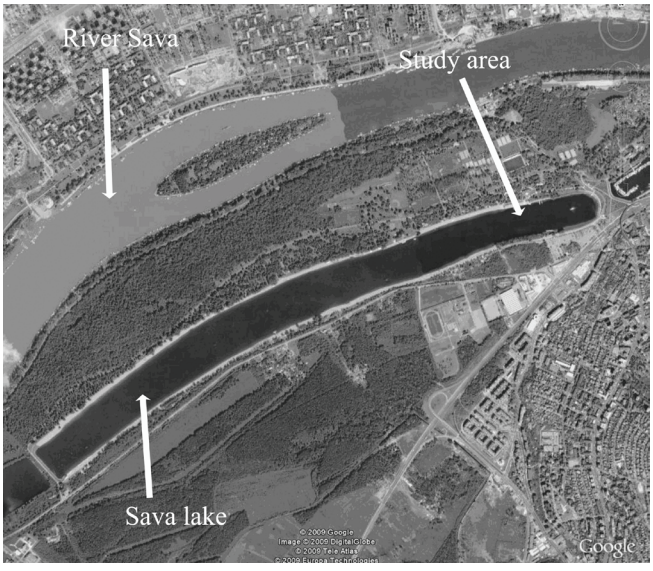

Figure 1: Satellite image of Sava Lake with the study area marked

There are 20 different fish species present in the lake. Relative to the total fish biomass in the lake, European perch is represented with 6.0% and black bullhead with 5.7%. According to (19) the total biomass of the European perch and black bullhead populations in the lake was 7.5 kg ha^{-1} and 9.5 kg ha^{-1}, respectively, while the annual production was 11.9 kg ha^{-1} and 15.2 kg ha^{-1}, respectively.

Sampling and sample preparation

All European perch and black bullhead specimens were sampled in March and September 2010. Samples were collected using 15 double fyke nets (8 mm mesh-size), which were left in the water for 3 nights and checked daily.

Nine European perch and 10 black bullhead specimens were collected and their total length (TL) and weight (W) were measured to the nearest 0.1 cm and 0.1 g accuracy, respectively. Individuals were anaesthetised by administering clove oil in the water until they were determined to be unconscious (i.e., by the loss of reflexes) (20). Specimens were consequently dissected with a plastic laboratory set. Samples of gills, muscle, and liver were quickly removed, washed with distilled water, and stored at -18°C prior to analysis. All animal procedures were in compliance with the EEC Directive (86/609/EEC) on the protection of animals used for experimental and other scientific purposes, and were approved by the Ethical Committee for the Use of Laboratory Animals of the Institute for Biological Research "Siniša Stanković", University of Belgrade.

Element analysis

The following elements were analysed: aluminium (Al), arsenic (As), boron (B), barium (Ba), cadmium (Cd), cobalt (Co), chromium (Cr), copper (Cu), iron (Fe), lithium (Li), manganese (Mn), molybdenum (Mo), nickel (Ni), lead (Pb), selenium (Se), strontium (Sr), and zinc (Zn). All samples were dried by Freeze Dryers Rotational-Vacuum-Concentrator, GAMMA 1-16 LSC, Germany, and sample portions between 0.2 and 0.5 g (dry weight) were subsequently processed in a microwave digester (speedwave™ MWS-3^{+}; Berghof Products + Instruments GmbH, Eningem, Germany), using 6 ml of 65% HNO_3 (Merck suprapure) and 4 ml of 30% H_2O_2 (Merck suprapure) at a food temperature program (100–170°C). After cooling to a room temperature, digested samples were diluted with distilled water to a total volume of 25 ml. The analysis was performed by inductively-coupled plasma optical spectrometry (ICP-OES; Spectro Genesis EOP II, Spectro Analytical Instruments DmbH, Kleve, Germany), comprising the assessment of concentrations of 17 metals expressed as μg g^{-1} dry weight (dw). The following wavelength lines of the ICP-OES analysis were used (nm): Al 394.401, As 189.042, B 249.773, Ba 233.527, Cd 228.802, Co 228.616, Cr 205.552, Cu 324.754, Fe 259.941, Li 460.289, Mn 259.373, Mo 202.095, Ni 231.604, Pb 220.353, Se 196.090, Sr 460.733, and Zn 206.191. The following detection limits were obtained during the analysis (mg l^{-1}): Al 0.00158, As 0.00282, B 0.000931, Ba 0.000531, Cd 0.000132, Co 0.00024, Cr 0.000366, Cu 0.000588, Fe 0.000562, Li 0.042, Mn 0.000403, Mo 0.000784, Ni 0.00114, Pb 0.00343, Se 0.00197, Sr 0.00138 and Zn 0.000391. The quality of the analytical process was controlled by the analysis of BCR-185R reference materials of bovine liver, as well as IAEA-336 lichen reference material. The concentrations found were within 90-115% of the certified values for all measured elements.

Statistical analysis

To compare heavy metal and trace element distribution and concentrations between European perch and black bullhead specimens, as well as between different tissues of the two species, the principal component analysis (PCA) was applied. To compare particular pairs of samples, the Mann-Whitney U test was used. In order to compare heavy metal and trace element concentrations in studied fish with maximum allowable concentrations (MAC) in fish meat for the utilization in human diet, established by the national legislation (21), concentrations were recalculated to the μg g^{-1} wet tissue weight (ww).

Results

The average total length of European perch and black bullhead specimens was 17.4 ± 1.9 cm and 19.6 ± 1.7 cm, respectively, while the average weight was 69.6 ± 25.1 g and 79.6 ± 21.9 g, respectively. Concentrations of B, Ba, Cd, Co,

Cr, Li, Ni, Pb, and Se were below the detection limits in all analysed samples, and consequently, concentrations of these elements were not subjected to statistical analysis. Concentration of Al was below the detection limit in muscle and liver, as well as of Fe and Mn in muscle of both fish species. Cu was detected only in black bullhead liver samples. Heavy metal and trace element concentrations in each of the three analysed tissues of the two fish species are presented in Table 1.

Results of the PCA conducted on gill samples indicated that the black bullhead samples were grouped based on the increased concentrations of Al, Fe, Sr, and Zn (Fig. 2). In muscle samples, European perch specimens were differentiated by higher concentrations of Sr (Fig. 3). In liver samples, black bullhead specimens were differentiated by higher Cu, Mn, and Zn concentrations, and European perch specimens by higher As, Mo, and Sr concentrations (Fig. 4).

Accumulation of the elements in gills had the following trend: Fe>Zn>Sr>Al>As>Mo>Mn in European perch, and Fe>Al>Zn>Sr>As>Mn>Mo in black bullhead. The trend of elemental accumulation in muscle was Sr>Zn>As>Mo in European perch, and Zn>Sr>As>Mo in black bullhead. Elemental ranking in the liver was Fe>Zn>Sr>As>Mo in European perch, and Fe>Zn>Sr>Cu>As>Mo>Mn in black bullhead. Results indicate that the distribution of investigated elements among different tissues had a consistent pattern among the two studied fish species.

Mann-Whitney U Test indicated that Fe and Zn concentrations in both liver and gills significantly differed ($p<0.05$) between the two fish species, as well as Al, Mn, and Sr in gills and As and Mo in liver (Table 1). Sr was the only element whose concentrations significantly differed between the two species in muscle.

The national MAC for Fe, prescribed by the National Regulation of the Republic of Serbia (for canned fish meat, 30.0 μg g^{-1} wet weight) (21), was exceeded in gills and liver, with average values of 33.9 and 42.7 μg g^{-1} ww in gills of European perch and black bullhead, respectively, and of 32.2 and 110.5 μg g^{-1} ww in liver of European perch and black bullhead, respectively. Arsenic concentrations exceeded the national MAC (for canned fish meat, 2.0 μg g^{-1} ww) and the lower limit set by FAO (0.1 μg g^{-1}) only in liver of European perch (3.96 μg g^{-1} ww). Concentrations of Cu and Zn were below the national MAC of 30 μg g^{-1} and 100 μg g^{-1}, respectively, in all analysed tissues and in both fish species. There is no national MAC established for Al, Mn, Mo, and Sr.

Table 1: Concentrations of chemical elements in different tissues of European perch and black bullhead (mean ± standard deviation). Concentrations are expressed as μg g^{-1} dw; significant differences between the two species within the same tissue are marked with an asterisk (*) ($p<0.05$ Mann-Whitney U Test); ND indicates the values below the detection limit

	Gills		Muscle		Liver	
	European perch	Black bullhead	European perch	Black bullhead	European perch	Black bullhead
Al	21.0 ± 37.4*	212 ± 65.6*	ND	ND	ND	ND
As	3.82 ± 0.54	4.83 ± 2.07	3.89 ± 0.30	4.16 ± 0.68	8.05 ± 4.01*	4.82 ± 1.80*
Cu	ND	ND	ND	ND	ND	10.91 ± 8.28
Fe	126 ± 53.0*	246 ± 84.7*	ND	ND	150.84 ± 141*	451 ± 276*
Mn	1.49 ± 1.07*	3.29 ± 2.02*	ND	ND	ND	2.37 ± 1.78
Mo	1.77 ± 0.27	2.30 ± 1.02	1.85 ± 0.16	1.99 ± 0.33	4.23± 2.08*	2.69 ± 0.90*
Sr	34.7 ± 6.42*	51.7 ± 11.4*	30.7 ± 4.60*	22.0± 3.59*	41.3 ± 21.7	25.5 ± 9.44
Zn	49.7 ± 10.1*	73.6 ± 9.99*	29.8 ± 8.26	31.5 ± 8.82	42.7 ± 15.0*	88.5 ± 16.2*

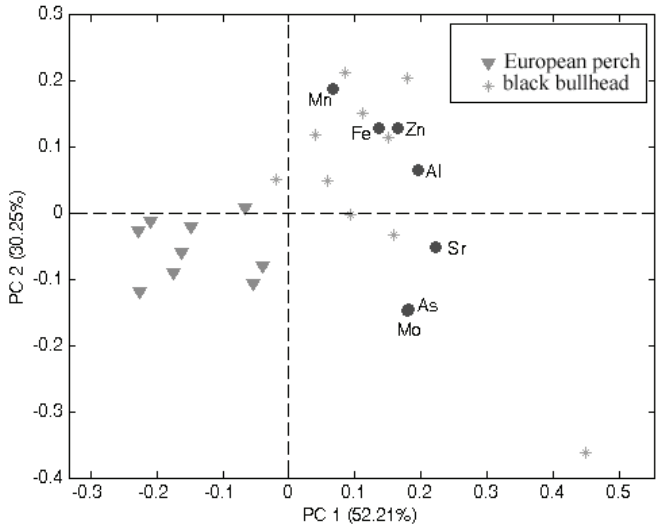

Figure 2: PCA of elemental concentrations in gills of European perch and black bullhead (untreated data were used as input variables)

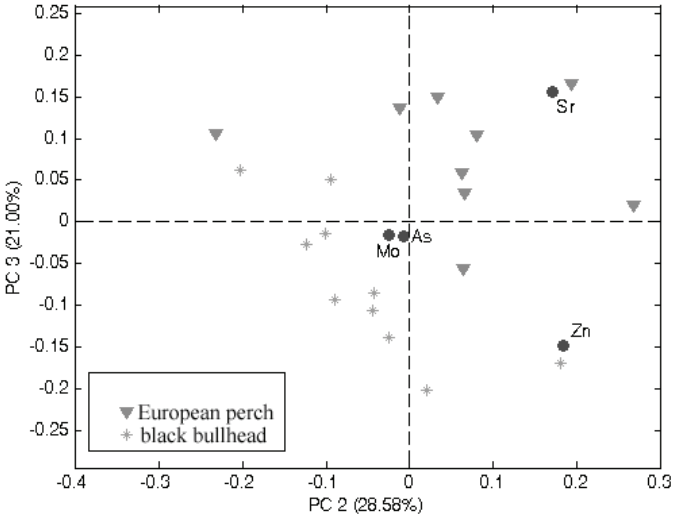

Figure 3: PCA of elemental concentrations in muscle of European perch and black bullhead (untreated data were used as input variables)

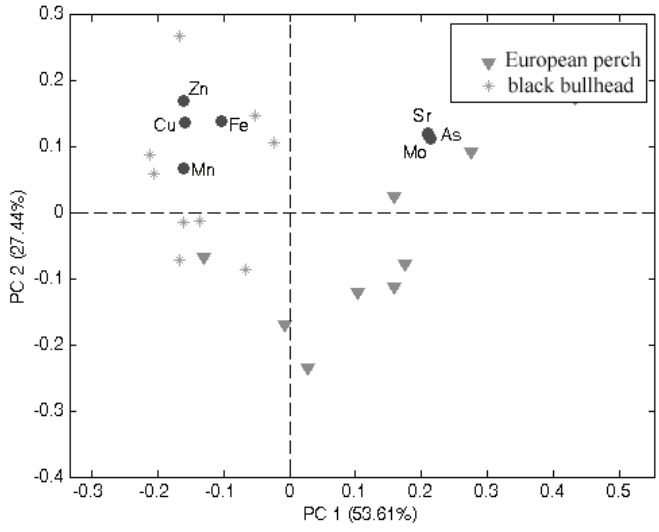

Figure 4: PCA of elemental concentrations in liver of European perch and black bullhead (untreated data were used as input variables)

Discussion

In the present study, elemental concentrations were the lowest in muscles and the highest in liver and gills, which are metabolically more active tissues. This is in line with the findings of other authors (11). Similar results obtained for a number of fish species show that muscle is not an active tissue in accumulating metals (22). As stated by (23), fish muscle tissue accumulates lower concentrations of metals because it is well protected by the activity of other organs.

Cu was below detection limits in muscle and gills of both fish species, which is in accordance with the findings of (24). Tendency of Cu to accumulate in liver, as is the case of black bullhead in the present study, has also been observed by other authors in several fish species (8,17). Concentration of Cu in European perch liver was below detection limits, which differs from the findings of other authors (16, 25). Tkatcheva et al. (25) have found high concentrations of Cu in European perch in the area where the level of Cu is unusually high due to the local geological features, while the area studied by (16) is significantly polluted and eutrophic. On the other hand, as shown by (26), Zn can inhibit the accumulation of Cu in animal tissues and, consequently, offer certain protection against its toxic effects.

Fe was not detected in muscle, but high concentrations were found in gills and liver of both fish species, which is similar to observations made in 20 fish species inhabiting various freshwater habitats in Lithuania (1). High Fe concentrations in fish liver were also reported by other authors (3,8,24). Lowest tendency of Fe to accumulate in muscle was observed by (21) as well.

Mn was detected only in gills of both species and in liver of the black bullhead, but in all cases in very low concentrations in comparison to other elements, which corresponds to findings of (24). The tendency of Mn to accumulate primarily in gills was also observed in perch, as well as in other fish species (3,23).

Determined concentrations of Mo were higher in all three tissues, both in European perch and black bullhead, than in sterlet (*Acipenser ruthenus*) (17), and in Pontic shad (*Alosa immaculata*) (15), where Mo concentrations were below the detection limits. Low Mo concentrations were also detected in muscle, gills, liver and gonads of five fish species from the Danube River (27), in muscle and liver of five fish species from the Persian Gulf (11), and in muscle of sturgeons from the Caspian Sea (28).

This study revealed that both fish species had high Zn concentrations in all three analysed tissues. However, they were below the national MAC of 100 μg g^{-1}(21), and also below the lower FAO limit of 40 μg kg^{-1} (31). Petkovšek et al. (9) also found that the overall concentration of Zn was the highest in comparison to other metals detected in gills, muscle, and liver of ten analysed fish species in three lakes in Slovenia. Although Zn is an essential element for human nutrition, it can be harmful when present in high concentrations (29). The mean Zn concentrations in analysed European perch and black bullhead specimens were lower in muscle than in gills, which is in line with the findings of (24), but contrary to the findings of (29).

European perch specimens had higher concentrations of As, Fe, Mo, Sr, and Zn in liver than in muscle, which is in line with the findings of (25), and (16), while Al, Cu, and Mn were below the detection limit in both tissues. There is a deficiency of the published data regarding heavy metal concentrations in black bullhead. The only available reference is the one by (30) who analysed elemental concentrations in homogenates of various fish species from Malibu Creek and Malibu Lagoon (Los Angeles, California), including black bullhead. According to their findings, assessed elements had the following trend: Fe>Zn>Al>Sr>Mo>As>Mn>Cu, which is in line with the results from the present study.

Similar heavy metal accumulation patterns in both species observed in the present study might be explained by a relatively similar diet of the two species. However, European perch had higher concentrations of Sr in muscle and of As, Mo, and Sr in liver, while black bullhead had higher concentrations of all analysed elements in gills, as well as of Cu, Fe, Mn, and Zn in liver (Table 1). This might be caused by different liver physiology and metabolic activity, habitat preferences, and predator-prey relationship between the two species, since recent field studies on Sava Lake indicated that the black bullhead preys on juvenile European perch specimens, while the opposite case was not recorded (Personal unpublished data). It is also well known that molluscs and crustaceans, which are important food components for subadult European perch

and for both juvenile and adult black bullhead, contain higher levels of several metals, particularly Cu and Zn, than do fish (16,25), which suggest that these prey organisms are the source of Cu and Zn in fish.

Conclusions

To conclude, concentrations of all analysed elements in both fish species were below MAC in all muscle samples; therefore, the consumption of these fish does not pose a risk to human health. Only Fe concentrations exceeded MAC in gills and liver of both fish species, and As in liver of European perch, which is in accordance with the previous studies on the Danube fish (17). Since fish species are good bioindicators of water contamination and pollution, the obtained results are important because of the large number of visitors that use the lake for recreational purposes. In addition, these two fish species are also used for human consumption.

Acknowledgements

The authors acknowledge the support by the Projects No. TR 37009 and No. 173045, funded by the Ministry of Education, Science and Technological Development of the Republic of Serbia. The authors would like to thank anonymous referees for providing helpful comments and suggestions that improved the quality of the paper.

References

1. Staniskiene B, Matusevicius P, Budreckiene B, Skibniewska KA. Distribution of heavy metals in tissues of freshwater fish in Lithuania. Pol J Environ Stud 2006; 15: 585–91.

2. FAO. Guidelines for risk based fish inspection. FAO Food and Nutrition Paper. Rome: FAO, 2009: 1–93. http://www.fao.org/docrep/011/i0468e/i0468e00.htm (Jan., 2014)

3. Yilmaz AB, Sangün MK, Yağlioğlu D, Turan C. Metals (major, essential to non-essential) composition of the different tissues of the three demersal fish species from İskenderun Bay, Turkey. Food Chem 2010; 123: 410–5.

4. Sures B, Steiner W, Rydlo M, Taraschewski H. Concentrations of 17 elements in the Zebra Mussel (*Dreissena polymorpha*), in different tissues of perch (*Perca fluviatilis*), and in perch intestinal parasites (*Acanthocephalus lucii*) from the subalpine Lake Mondsee, Austria. Environ Toxicol Chem 1999; 18: 2574–9.

5. Reid SD. Molybdenum and chromium. In: Wood MC, Farrell AP, Braune CJ, eds. Fish physiology. Vol. 31A: homeostasis and toxicology of essential metals. London: Elsevier, 2011: 375–415.

6. Pourang N. Heavy metal bioaccumulation in different tissues of two fish species with regards to their feeding habits and trophic levels. Environ Monit Assess 1995; 35: 207–19.

7. Farag AM, Stansbury MA, Hogstrand C, MacConnell E, Bergman HL. The physiological impairment of free-ranging brown trout exposed to metals in the Clark Fork River, Montana. Can J Fish Aquat Sci 1995; 52: 2038–50.

8. Jezierska B, Witeska M. The metal uptake and accumulation in fish living in polluted waters. In: Twardowska I, Allen HE, Haggblom MM, Stefaniak S, eds. Viable methods of soil and water pollution monitoring, protection and remediation. New York: Springer, 2006: 107–14.

9. Petkovšek SAS, Grudnik ZM, Pokorny B. Heavy metals and arsenic concentrations in ten fish species from the Šalek lakes (Slovenia): assessment of potential human health risk due to fish consumption. Environ Monit Assess 2012; 184(5): 2647–62.

10. Kenšová R, Čelechovská O, Doubravová J, Svobodová Z. Concentrations of metals in tissues of fish from the Věstonice reservoir. Acta Vet Brno 2010; 79: 335–45.

11. Agah H, Leermakers M, Elskens M, Fatemi SMR, Baeyens W. Accumulation of trace metals in the muscle and liver tissues of five fish species from the Persian Gulf. Environ Monit Assess 2009; 157: 499–514.

12. Declerck S, Louette G, De Bie T, De Meester L. Patterns of diet overlap between populations of non-indigenous and native fishes in shallow ponds. J Fish Biol 2002; 61: 1182–97.

13. Ceccuzzi P, Terova G, Brambilla F, Antonini M, Saroglia M. Growth, diet, and reproduction of Eurasian perch *Perca fluviatilis* L. in Lake Varese, northwestern Italy. Fisheries Sci 2011; 77(4): 533–45.

14. Leunda PM, Oscoz J, Elvira B, Agorreta A, Perea S, Miranda R. Feeding habits of the exotic black bullhead *Ameiurus melas* (Rafinesque) in

the Iberian peninsula; first evidence of direct predation on native fish species. J Fish Biol 2008; 73: 96–114.

15. Višnjić-Jeftić Ž, Jarić I, Jovanović Lj, et al. Heavy metal and trace element accumulation in muscle, liver and gills of the Pontic shad (*Alosa immaculata* Bennet 1835) from the Danube river (Serbia). Microchem J 2010; 95(2): 341–4.

16. Szefer P, Domagala-Wieloszewska M, Warzocha J, Garbacik-Wesolwska A, Ciesielski T. Distribution and relationship of mercury, lead, cadmium, copper and zinc in perch (*Perca fluviatilis*) from the Pomeranian bay and Szczecin lagoon, southern Baltic. Food Chem 2003; 81: 73–83.

17. Jarić I, Višnjić-Jeftić Ž, Cvijanović G, et al. Determination of differential heavy metal and trace element accumulation in liver, gills, intestine and muscle of sterlet (*Acipenser ruthenus*) from the Danube river in Serbia by ICP-OES. Microchem J 2011; 98: 77–81.

18. Blaženčić J. Florističke karakteristike makrofitske vegetacije Savskog jezera kod Beograda. Glasn Inst Bot Bot Bašte Univ Beogr 1995; 29: 167–73.

19. Hegediš A, Nikčević M, Mićković B. Fisheries management plan for the fishing area „Serbia-West“ for the period 2008-2012. Beograd: Institute for multidisciplinary research, University of Belgrade, Serbia 2008: 82–7.

20. AVMA Guidelines for the euthanasia of animals: 2013 edition. Schaumburg: American Veterinary Medical Association, 2013, version 2013.0.1 https://www.avma.org/KB/Policies/Documents/euthanasia.pdf. (4. 9. 2013)

21. Pravilnik o količinama pesticida, metala i metaloida i drugih otrovnih supstancija, hemioterapeutika, anabolika i drugih supstancija koje se mogu nalaziti u namirnicama. Sl List SRJ 1992; br. 5/92, 11/92 - ispr. i 32/2002

(Regulation on quantity of pesticides, metals, metalloids, and other toxic substances, chemotherapeutics, anabolics, and other substances which can be found in food. Official Gazzette of SRJ 5/92).

22. Yilmaz F, Özdemir N, Demirak A, Tuna AL. Heavy metal levels in two fish species *Leuciscus cephalus* and *Lepomis gibbosus*. Food Chem 2007; 100: 830–5.

23. Rajkowska M, Wechterowicz Z, Lidwin-Kazmerkiewicz M, Pokorska K, Protasowicki M. Accumulation of selected metals in roach (*Rutilus rutilus* L.) from West Pomerian lakes. Ecol Chem Eng 2008; 15(1/2): 119–24.

24. Tekin-Özan S, Kir I. Comparative study on the accumulation of heavy metals in the organs of tench (*Tinca tinca* L.1785) and plerocercoids of its endoparasite *Ligula intestinalis*. Parasitol Res 2005; 97: 156–9.

25. Tkatcheva V, Holopainen IJ, Hyvärinen H. Heavy metals in perch (*Perca fluviatilis*) from the Kostomuksha region (North-western Karelia, Russia). Boreal Environ Res 2000; 5: 209–20.

26. Bireš J, Dianovský J, Bartko P, Juhásová Z. Effects on enzymes and the genetic apparatus of sheep after administration on samples from industrial emissions. Biometals 1995; 8: 53–8.

27. Lenhardt M, Jarić I, Višnjić-Jeftić Ž, et al. Concentrations of 17 elements in muscle, gills, liver and gonads of five economically important fish species from the Danube river. Knolw Managt Aquat Ecosyst 2012; 407: e2 (10 p.) http://www.kmae-journal.org/articles/kmae/abs/2012/04/kmae120089/kmae120089.html (Jan. 2014)

28. Agusa T, Kunito T, Tanabe S, Pourkazemi M, Aubrey DG. Concentration of trace elements in muscle of sturgeons in the Caspian sea. Mar Pollut Bull 2004; 49(9/10): 789–800.

29. Stanek M, Stasiak K, Janicki B, Bernacka H. Content of selected elements in the muscle tissue and gills of Perch (*Perca fluviatilis* L.) and water from a Polish lake. Pol J Environ Stud 2012; 21(4): 1033–8.

30. Moeller A, MacNeil SD, Ambrose RF, Que Hee SS. Elements in fish of Malibu creek and Malibu lagoon near Los Angeles, California. Mar Pollut Bull 2003; 46: 424–9.

31. Nauen CE, FAO. Compilation of legal limits for hazardous substances in fish and fishery products. Rome: Food and Agriculture Organization of the United Nations, 1983. (FAO Fishery Circular, No. 764)

KONCENTRACIJE ELEMENTOV V RAZLIČNIH TKIVIH EVROPSKEGA OSTRIŽA IN ČRNE PISANKE IZ JEZERA SAVA (SRBIJA)

M. Jaćimović, M. Lenhardt, Ž. Višnjić-Jeftić, I. Jarić, Z. Gačić, A. Hegediš, J. Krpo-Ćetković

Povzetek: Preučili smo porazdelitev 17 kemijskih elementov v škrgah, mišicah in jetrih evropskega ostriža (Perca fluviatilis) in črnega somiča (Ameiurus melas) iz jezera Sava (Srbija). Želeli smo ugotoviti vzorce bioakumulacije glede na vrstno specifično prehrano in glede na nivo v prehranski verigi. Koncentracije Ba, Cd, Co, Cr, Li, Ni, Pb, B in Se so bile pod mejo detekcije. Koncentracije Al, Fe, Mn, Sr in Zn so bile višje v škrgah črnega somiča. As, Mo in Sr so bile višji v jetrih evropskega ostriža; Fe in Zn pa v jetrih črnega somiča. V mišicah je bila edina razlika med vrstama v koncentraciji Sr. Baker smo ugotovili samo v jetrih črnega somiča. Glede na to, da nismo odkrili bistvenih razlik v koncentraciji merjenih elementov med vrstama, sklepamo, da imata obe relativno podobno prehrano. Razlika v koncentraciji elementov v škrgah pa nakazuje, da imata vrsti različne preference do življenjskega okolja.

Ključne besede: težka kovina; onesnaževanje; ostriži; ameriški somič; Donava

Slov Vet Res 2015; 52 (2): 67-74
UDC 638.121.2:638.144:612.4.09:612.33

Original Scientific Article

CHARACTERISTICS OF HYPOPHARYNGEAL GLANDS IN HONEYBEES (*Apis mellifera carnica*) FROM A NURSE COLONY

Maja I. Smodiš Škerl*, Aleš Gregorc

Agricultural institute of Slovenia, Hacquetova ulica 17, 1001 Ljubljana, Slovenia

*Corresponding author, E-mail: maja.smodis.skerl@kis.si

Summary: The development and size of hypopharyngeal glands (HPGs) in workers sampled from the nurse colony was compared to workers from the control queen-right honeybee colony. The diameter of the acini in workers (age 1 to 30 days) from the nurse colony ranged from 109.2 to 180.9 µm, and in workers of the same age from the control colony was between 100.8 and 158.2 µm. We found that nurses from the nurse (cell builders) colonies aged 15 to 27 days had significantly larger acinar diameter ($p<0.0001$) than the workers in the control colonies of the same age. We described the morphological and histological characteristics of the HPGs in nurse workers aged 1 to 27 days and found that HPGs secretion in brood feeding nurses was extended in comparison to workers from the control colony. Moreover, we described the HPGs in a worker pupa before the emergence and in winter bees from the control colony. Results show that HPGs in worker pupae consist of clusters of irregularly shaped secretory acini. Cell cytoplasm is not structured and is homogeneous, nuclei are dense and oval in shape. Winter bees had hypertrophied HPGs and cells containing numerous vesicles accumulating secretion. We found larger acini with a dense structure and milky-white colour. Physiological function of the glands and age related tasks of nurse worker bees is also discussed.

Key words: acinar diameter; age; morphology; nurse bee; winter bee; worker pupa

Introduction

Hypopharyngeal glands (HPG) produce and secrete the components of royal jelly which is the most important food for brood and queen. In young workers, the glands are well developed with large actively secreting acini. Development of HPGs, which produce royal jelly, i.e. food for larvae, is of great importance in the quality queen rearing. HPGs are located in a head of a honeybee worker and a queen but only develop in workers (1, 2). Active secretion reaches its peak in nurse-workers at the age of 6 to 13 days and HPG were mostly studied in workers. Active secretion was observed in nurse workers, newly-emerged bees and older workers (3). Reduced glandular activity was detected using a histochemical method of localising acid phosphatase activity in cells of adult workers and queens, despite the fact that the glands were anatomically in the regression phase (4). Furthermore, comparing the gland structure and morphology of *Polistes versicolor* (*Hymenoptera, Vespidae*) and other groups of Hymenoptera, HPGs in different age groups of P. versicolor have

Received: 8 July 2014
Accepted for publication: 25 November 2014

similar morphological characteristics with the exception in the size of secretory cells that differ between the individuals and does not depend on age (5). The reason for such age independence is a hierarchy which occurs in a linear way in *Polistes* without morphological differences between castes.

The HPGs glands in the honeybee are a paired organ, located in the head of the worker bee, in front of the brain between the compound eyes. The ducts open into the sub-oral part of the hypopharynx. Each of the glands is composed of numerous small oval bodies or acini, short parts attached to axial or terminal secretory duct. Each acinus is determined by 10 to 15 individual cellular bodies and each cell is connected to the axial duct via a thin duct (6). The gland size increases and decreases with age of a worker. In newly-emerged workers the glands are inactive and the secretory vesiculi develop by the age of 3 days (7). Six-day old bees produce secretion in the glands and at the age of 9 days the glands secrete the enzymes and cooperate in royal jelly production (8). However, at the age of 15 days secretion activity increases and the cells already start to form lysosomes which are involved in the degeneration processes (7). In winter, the bees' glands are hypertrophied and it is assumed that the secretion is stored till spring. Glands activate in the presence of a young brood and are less active in protein synthesis in comparison to middle sized glands of young workers (9). Younger summer workers with larger acini actively produce proteins more than older foragers, which have smaller gland size (10), with clear signs of structural degeneration and regression indicating cell death (11). Glandular development and royal jelly production depend on protein vitellogenin that slows down aging in workers and queens (12), but has an effect on HPGs only in nurse workers (13). In previous research, the ultrastructural changes during HPGs development were described at different age groups of bees (2, 7, 9, 14, 15, 16, 17). Rough endoplasmic reticulum in the cells, characteristic for protein synthesis, starts to expand as the worker emerges and the maximum size is reached in nurse workers, and decreases in foragers. Intracellular ducts, which function to store and transport secretion material, expand from the space between the endocuticule and gland cell membrane into the secretion vesicules (2). Within septa of the secretory cell there are filamentous actin (F-actin)-decorated tubular structures (actin rings) connected to an extracellular ductus (18). The authors speculate that the function of the actin rings is important for the secretion process. Foragers have smaller amounts of proteins in the HPGs in comparison to older workers, which have the ability to reactivate gland secretion. This only happens as a response to needs inside and/or outside the brood nest (2).

Histological structure in the HPGs was only presented in a normal queen-right colony, therefore we wanted to analyse morphological and histological changes in the HPGs in nurse bees of a different age in a nursing colony and compare the size of the acini with the HPGs in a normal, control colony. Moreover we described the HPGs in a worker pupa and winter bees.

Material and methods

For the experiment, two colonies were established, a normally developed honeybee colony as a control and a nurse colony, both without any visible disease symptoms. The nurse colony was obtained with plenty of young nurse workers. The experiment was conducted in the experimental apiary of the Agricultural Institute of Slovenia in Senično situated in the Gorenjska region. Worker honeybees (*A. m. carnica*) were obtained as a mixture from three colonies. Bees emerged from their brood comb in an incubator at 34.5 °C (±1.0) and 60 % relative humidity. Around 100 newly emerged workers (age 0–24 hrs) were marked on the thorax with a marker of the same colour to define their age and inserted into the control colony. The procedure with introducing the newly emerged bees, marked with the same colour on the same day into the honeybee colony, was repeated every three days. At the beginning of the experiment, the nurse colony of two hive boxes was established, with a queen excluder in the middle. The queen was kept in the lower box. Into the upper box we added a honey comb, a comb with bee bread and a comb with a sealed brood arranged from both outer sides. Finally, approx. 2 kg of young nurse workers were added into the upper box and among these bees approximately 100 marked young workers were added into the box. The presence of workers and sealed brood was checked and the combs with honey or pollen were replaced. When the first marked workers were inserted into the colonies, 10 larvae (aged

12–24 h) were grafted and inserted into the middle of the upper nest box of the nurse colonies. The next and consecutive insertion of grafted larvae was performed on the third, eighth and tenth days after the first insertion. During the same periods, approx. 100 newly emerged and marked bees were put into each of the control and nurse colonies.

Bee sampling

Nurse bees at different ages, from 1 to 30 days, including nurse bees feeding queen larvae in the nurse colony, were sampled regularly at the time of introduction into the colonies and every five days thereafter. Three workers were sampled from each age and experimental group. Worker pupae with dark coloured compound eyes, aged around 17 days, were sampled from the brood comb cells. In November of the same season, winter bees of unknown age from the control colony were also sampled.

Dissection of the glands

Bees were immobilized with CO2 and the head in Hyes' solution (NaCl 9.0 g, KCl 0.2 g, CaCl 0.2 g, $NaHCO_3$ 0.1 g, 1 l distilled water, pH 8.5) was fixed with two entomological needles on a rubber base (Xantopren® L blue and Activator universal, Heraeus Kulzer, Germany) in a Petri dish. Dissection was performed using the stereomicroscope (SterREO Discovery.V12, Zeiss). The external chitinous exoskeleton of the facial region of the head was removed between the compound eyes, and prepared for the further histological procedure.

Preparation of the tissue for histological analyses

The dissected tissue was fixated in 10% Formaldehyde solution (100 ml Formaldehyde solution, min 37 %; 8,5 g NaCl; tap water; 0.165 M, pH 7.1) for 24 hours (±1), dehydrated in different concentrations of alcohol (70%, 90%, 100%, 100% alcohol; Ethanol 96 vol. %; demineralised water) and in xylene for 24 hours (±1) each time. Samples were moved into a plastic histosettes, put into an incubator at 60 °C with three glass tubes containing xylene and wax (3:1, 1:1 and 1:3, xylene:wax), for 24 hours each time. Samples were transferred in the glass tube containing wax and incubated for 24 hours (±1) and finally in the fresh wax for 6 to 12 hours. The samples were then embedded in wax using metal moulds and cooled on the cold plate. Sections of 5 µm were then cut on a microtome, floated on distilled water (42 °C) and collected on cleaned slides. The tissue on the slides was first dewaxed with xylene 3 times for 5 minutes, rehydrated in 100% alcohol (Ethanol 96 vol %) 3 times for 3 minutes and then stained with hematoxylin and eosin. A drop of water-soluble fluid (Faramount Aqueous Mounting Medium, Dako) was put on a slide with a stained tissue and covered with cover glass. The prepared material was analysed using light-microscope.

Acini measurements

Morphological measurements of the gland lobes (acini) in nurse workers, pupae and winter bees were performed 'in vivo' using stereomicroscope (SterREO Discovery.V12, Zeiss) and camera (Zeiss). The images were stored and later measured using the program AxioVision Rel. 4.6. In three workers of the same age, diameters of 30 randomly selected acini were measured perpendicular to the longer axis of the oval acinus. The shape of an acinus is oval, so only the length of the shorter axis was measured and used for calculation.

Data analysis

Data were statistically evaluated with SPSS version 13.0 (SPSS Inc.; Chicago, IL, USA). Basic statistical parameters were calculated with Means and Descriptive. Significant differences in acini diameter were calculated using One-way ANOVA, with a filter as a cell bar introduction (1 to 3) and type of the colony (nurse colony, control colony). Data of differently aged workers were compared. Mean acini diameter of HPGs was compared between workers from the nurse colony and the control colony, using One-way ANOVA with age as a factor and further compared with cell bar introduction as a factor. For data testing Scheffe test was applied. Acini diameter in HPG of pupae and winter bees was measured. Basic statistical parameters were calculated with Means and Descriptive.

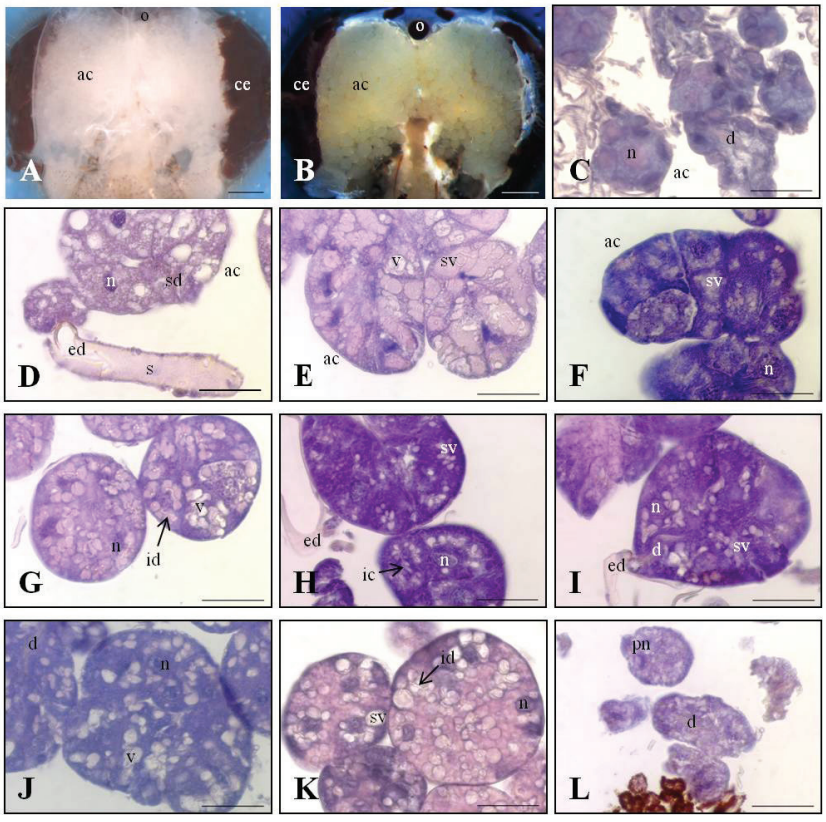

Figure 1: A - HPGs in honeybee pupae in vivo are transparent and lobular structure is not clearly seen. B - In winter bees HPGs with a milky-white colour, lobular structure with acini (ac), compound eye (ce) and ocellus (o) can be seen. Scale bar 0.5 mm. Histological section of the HPG gland acini, stained with Hematoxylin and eosin. Acini in worker pupa (C) and winter bee (D and E). Acini of (F) 1-day, (G) 3-day old workers from nurse colony and (H) 6-day, (I) 9-day and (J) 12-day-old workers from control colony. Acini of 18 day-old worker from (K) nurse colony and (L) control colony. Ac – acinus, n – nuclei of the gland cell, v – vesicle, sv – secretory vesicle, sd – secretory duct, s - secret, id – intracellular duct, ed – excretory duct, d – ducts, pn – picnotic nuclei. Scale bar 50 μm

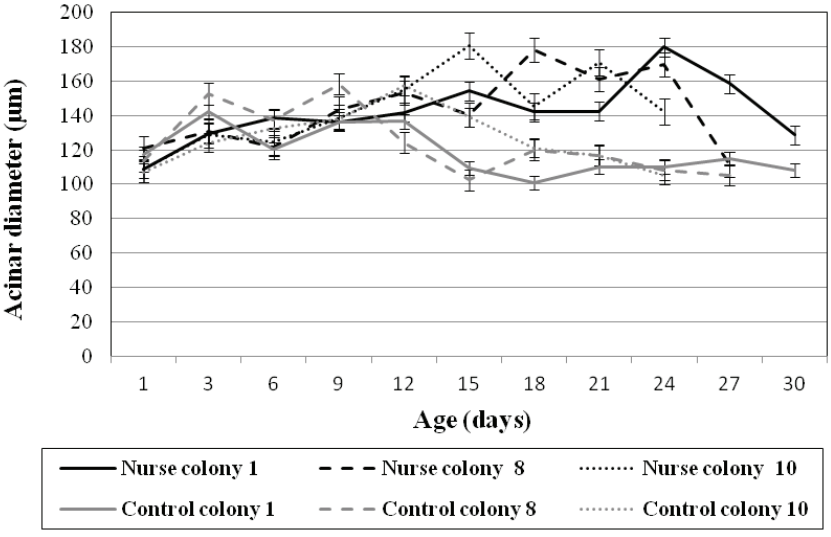

Figure 2: Average acini diameter (± SD) of the HPGs in 1 to 30 days old workers from the nurse colony and normally developed (control) honeybee colony which was not included in queen brood feeding. Newly emerged marked workers and grafted larvae were inserted into the nurse colony on day 1 (Nurse colony 1), 8 (Nurse colony 8) and 10 (Nurse colony 10). Newly emerged workers were marked and inserted into the control colony as well

Results

Morphological characteristics of hypopharyngeal glands *in vivo*

HPGs in worker pupa consist from transparent acini (Fig. 1A). In late summer and in early fall, "long-lived" workers accumulated body fat and the morphological structure of the HPGs starts to change. In these workers we found large acini with a dense structure and milky-white colour (Fig. 1B).

The acini diameter in workers sampled in the nurse colony aged from 1 to 30 days, ranged from 109.2 to 180.9 μm, and acini in workers from the control colony ranged between 100.8 and 158.2 μm (Fig. 2). Acini diameter of 15 and 27 day-old (1st

cell bar introduction) nurses and acini diameter of 15, 18, 21 and 24 day-old nurses (2nd and 3rd cell bar introduction) originated from the nurse colony, was significantly larger in comparison to the acini diameter in workers originating from the control colony ($p < 0.0001$).

Morphological characteristics of acini

In worker pupae (from a control colony) clusters of irregularly shaped secretory acini were found. Cytoplasm is not structured and is homogeneous, nuclei are dense and oval (Fig. 1C). In winter bees, there are numerous large secretory vesicles present in the glandular cells. The size of the vesicles varied between 1.5 and 22.81 μm (winter bees from the control colony, n=3; 30 acini per bee were measured). Cell nuclei are regularly or irregularly shaped and dense, with a dense secretory material visible in the ducts (Fig. 1D).

One-day-old workers have small-sized glands, homogenous and well structured cell cytoplasm. Nuclei are large and spherical with an evident chromatin granulation and smaller vesicles around the nucleus (Fig. 1E). In three-day-old bees, vesicles are larger, especially in workers from the nurse colony, and there is secretion present in vesicles and ducts (Fig. 1F). Workers from the nurse and control colony have similarly larger acini at 6 to 12 days of age and there are numerous secretory vesicles in cell cytoplasm (Fig. 1G, H and I). In 12-day-old workers from the control colony, cell nuclei already have irregular shape, some are picnotic but in the majority of the nuclei the chromatin is still evidently granulated (Fig. 1J). In 18-day-old workers from the nurse colonies, acini are large and indicative for active secretion (Fig. 1K). Acini in workers of the same age from the control colony are small in the size, cell cytoplasm is unstructured, without secretion. There are picnotic nuclei of irregular shape (Fig. 1L), and some of the nuclei are dilated.

Discussion

HPGs start to develop in worker pupae about a week before emergence (19) and continue after bees emerge from the brood comb, changing structure until they die. In summer bees, glands are flexible and can reactivate the HPG activity when needed. In our research, we demonstrated the ability of glands to prolong their activity and enlarge their size which does not depend on the age of the workers. When the honeybee colony has a need of rearing a new brood or new queens, as in our case, workers stay in the hive for a longer period and feed larvae. In the meantime, the acini size increases after the age of 12 days and, as shown in our study, decreases after the age of 24 days when workers usually forage. This contrasts with previous observations which found the peak of gland secretion is at the age of 6 days (20, 7). According to our findings it is evident that workers have the ability to increase glandular activity, and that older nurse workers from the nursing colony, compared with workers from the normal (control) colony, have well developed HPGs with larger acini. Gland cells have numerous secretory vesicles accumulating secretion, they actively secrete and cell nuclei remain spherical containing granulated chromatin. Glands in older forager bees, as comparable to our workers from a normal colony can be reactivated when needed and start to secret (2). Acini size in workers from nurse and honeybee colonies is correlated with their activity, which is in accordance with the previous research (20, 7).

We found that young nurse workers have larger glands when there is an abundance of queen cells in the nursing colony compared to the nurses from the control colony. In addition to that, the nurses from the breeder aged over 15 days had a larger acini diameter than the same-aged nurses from the control colony. According to the morphological and histological findings, the glands have an active secretion at the age of 27 days and it indicates that the older workers keep their task as nurses and continue intensive brood feeding.

When the gland cells are not developed, they are less productive than the glands with the middle-sized acini (10). The structure of the HPGs changes with the age of individual worker bees and the tasks in the hive. The division of labour and related changes in the organism are called the age polyethism (21, 7). We found that nurse workers stayed in the hive for a longer time in comparison to workers in normal, control colonies and fed the brood. The queen was present in the nursing colony, but separated with the queen excluder. It is possible that the presence of the

queen secreting mandibular pheromone and young larvae in queen comb cells had an effect on the workers to remain in the nest and feed the queen brood. It was also important to have a sufficient number of young nurse workers in the nursing colony. HPGs have flexible secretion activity which depends on the needs of the brood rearing (22). Nurse workers have also larger acini in the active phase of secretion. Glandular acini remain enlarged in winter bees (9). Around the cell nuclei there are numerous secretory vesicles and secretion containing carbon hydrates (23). In young worker bees, secretory vesicles appear in the gland cells. At the age of 6 days, the peak amount of accumulated secretion is found in the secretory vesicles (7). However, later with increasing bee ages the size of the acini decreases and cells still contain some vesicles. It was found that at the age of 18 days the ultrastructure of the glands shows electronic dense secretion (7). After a worker emerges from the comb cell, the endoplasmatic reticulum (ER) starts to expand in the gland cells and increases when the worker feeds the brood. Later on, when workers age, it vigorously decreases. In fact, the proteins are intensively synthesized in younger workers but their productivity is decreasing with age. Knecht and Kaatz (2) suggest that the reduced activity of granular ER also decreases the size of the acini and secretory vesicles.

In regression processes of glands, the juvenile hormone (JH) increases and workers consequently begin to forage. Young workers start to forage after they were topically treated with JH (24) as was confirmed with the high concentration of JH in the haemolymph of foragers (25, 21), additionally the effect of diet on the HPG development is also confirmed (26). Le Conte et al. (27) suggested that the brood pheromone is a primary regulator of the behavioural development in workers and thus we can explain why workers remain for a prolonged period of time in the area with the queen brood. When a colony is not able to provide sufficient amount of nurse workers, the older workers change their tasks and start taking care of the brood (21).

To produce high quality royal jelly and to breed vital honeybee queens, one must consider the technology of breeding, pasture, technology of feeding and diet supplements, and also the presence of pathogens, i.e. honeybee viruses (28) and *Nosema* spp. (29). HPGs are a flexible organ in young worker bees and are able to actively respond to the needs of the colony, which is very important for brood rearing in swarms or queen supersedure, in periods of inclement weather conditions, as well as for massive queen breeding at the breeding stations.

Acknowledgements

We thank Vesna Lokar for her help with breeding queens, collecting samples and assisting with picture formation and to Marjan Kokalj for his technical support. This work was supported by the Slovenian Ministry of Education, Science and Sport and the Ministry of Agriculture and the Environment (Research programme P4-0133; project No. V4-0484).

References

1. Crailsheim K, Stolberg E. Influence of diet, age and colony condition upon intestinal proteolytic activity and size of the hypopharyngeal glands in the honeybee (*Apis mellifera* L.). J Ins Physiol 1989; 35: 595–602.

2. Knecht D, Kaatz HH. Patterns of larval food production by hypopharyngeal glands in adult worker honey bees. Apidologie 1990; 21: 457–68.

3. Costa RAC, Cruz - Landim C. Comparative study of the ultrastructure and secretory dynamic of hypopharyngeal glands in queens, workers and males of *Scaptotrigona postica* Latreille (Hymenoptera, Apidae, Meliponinae). Biocell 2000; 24: 39–48.

4. Costa RAC, Cruz - Landim C. Distribution of acid phosphatases in the hypopharyngeal glands from workers, queens and males of a Brazilian stingless bee *Scaptotrigona postica* Latreille: An ultrastructural cytochemical study. Histochem J 2001; 33: 653–62.

5. Britto FB, Caetano FH, de Moraes RLMS. Comparative analysis of morphological, structural and morphometric patterns of *Polistes versicolor* (Olivier) (Hymenoptera: Vespidae) hypopharyngeal glands. Neotrop Entomol 2004; 33: 321–6.

6. Snodgrass RE. Anatomy of the honey bee. London: Cornell University Press, 1984: 334.

7. Deseyn J, Billen J. Age-dependent morphology and ultrastructure of the hypopharyngeal gland of *Apis mellifera* workers (Hymenoptera, Apidae). Apidologie 2005; 36: 49–57.

8. Sasagawa H, Sasaki M, Okada I. Hormonal control of the division of labor in adult honeybees (*Apis mellifera* L.). I. Effect of methoprene on corpora allata and hypopharyngeal gland, and its α-glucosidase activity. Appl Entomol Zool 1989; 24: 66–77.

9. Huang ZY, Otis GW, Teal PEA. Nature of brood signal activating the protein synthesis of hypopharyngeal gland in honey bees *Apis mellifera* (Apidae: Hymenoptera). Apidologie 1989; 20: 455–64.

10. Cruz - Landim C, Hadek R. Ultrastructure of *Apis mellifera* hypopharyngeal gland. In: Proceedings of the 6th Congress of International Union for the Study of Social Insects. Switzerland Bern, 1969: 121–30.

11. Silva de Moraes RL, Bowen ID. Modes of cell death in the hypopharyngeal gland of the honey bee (*Apis mellifera* L.). Cell Biol Int 2000; 24: 737–43.

12. Seehuus SC, Norberg K, Gimsa U, Krekling T, Amdam GV. Reproductive protein protects sterile honeybee workers from oxidative stress. Proc Natl Acad Sci U S A 2006; 103: 962–7.

13. Engels W. Extra-oocytic components of egg growth in *Apis mellifera*. I. Trophocytic uptake of ribonucleic acid. Insectes Soc 1968; 15: 271–88.

14. Beams HW, King RL. The intracellular canaliculi of the pharyngeal glands of the honeybee. Biol Bull 1933; 64: 309–14.

15. Beams HW, Tahmisian TN, Anderson E, Devine RL. An electron microscope study on the pharyngeal glands of the honeybee. J Ultrastruct Res 1959; 2: 155–70.

16. Painter TS, Biesele JJ. The fine structure of the hypopharyngeal gland cell of the honey bee during development and secretion. Proc Natl Acad Sci U S A 1966; 55: 1414–9.

17. Halberstadt K. Elektrophoretische untersuchungen zur sekretionstatigkeit der hypopharynxdruse der honigbiene (*Apis mellifera*). Insectes Soc 1980; 27: 61–77.

18. Kheyri H, Cribb BW, Reinhard J, Claudianos C, Merritt DJ. Novel actin rings within the secretory cells of honeybee royal jelly glands. Cytoskeleton (Hoboken) 2012; 69(12): 1032–9

19. Theophilus SP, Biesele JJ. The fine structure of the hypopharyngeal gland cell of the honey bee during development and secretion. Proc Natl Acad Sci U S A 1966; 55: 1414–9.

20. Hrassnig N, Crailsheim K. Adaptation of hypopharyngeal gland development to the brood status of honeybee (*Apis mellifera* L) colonies. J Ins Physiol 1998; 44: 929–39.

21. Robinson GE. Regulation of honey bee age polyethism by juvenile hormone. Behav Ecol Sociobiol 1987; 20: 329–38.

22. Free JB. Hypopharyngeal glands development and division of labour in honey bee (*Apis mellifera* L.) colonies. Proc R Entomol Soc Lond B 1961; 36: 5–8.

23. Suwannapong G, Chaiwongwattanakul S, Benbow ME. Histochemical comparison of the hypopharyngeal gland in *Apis cerana* Fabricius, 1793 workers and *Apis mellifera* Linnaeus, 1758 workers. Hindawi pulishing corporation Psyche 1910; 1–7

24. Gracioli LF, Silva de Moraes RLM. Juvenile hormone promotes changes in the expression of hypopharyngeal gland proteins of worker *Apis mellifera* (Hymenoptera, Apidae). Sociobiology 2002; 40: 443–8.

25. Jaycox ER. Behavioral changes in work honey bees (*Apis mellifera* L.) after injection with synthetic hormone (Hym., Apidae). J Kansas Entomol Soc 1976; 49: 165–70.

26. Furquim KCS, Camargo - Mathias MI, Silva de Moraes RLM. Morphological modifications induced by an artificial diet on the hypopharyngeal glands of *Apis mellifera* (Hymenoptera, Apidae) during their degenerative process. Sociobiology 2004; 43: 279–93.

27. Le Conte Y, Mohammedi A, Robinson GE. Primer effects of a brood pheromone on honeybee behavioural development. Proc R Soc Lond B 2001; 268: 163–8.

28. DeGrandi - Hoffman G, Chen Y, Huang E, Huang MH. The effect of diet on protein concentration, hypopharyngeal gland development and virus load in worker honey bees (*Apis mellifera* L.). J Insect Physiol 2010; 56: 1184–91.

29. Liu TP. Ultrastructural analysis on the gland secretion in the extracellular ducts of the hypopharyngeal glands of the honeybee infected by *Nosema apis*. Tissue Cell 1990; 22: 533–40.

ZNAČILNOST HIPOFARINGEALNIH ŽLEZ PRI KRANJSKI MEDONOSNI ČEBELI (*Apis mellifera carnica*) IZ VZREJNE ČEBELJE DRUŽINE

M. I. Smodiš Škerl, A. Gregorc

Povzetek: V raziskavi smo primerjali velikost hipofaringealnih ali krmilnih žlez (HPG) pri delavkah, ki smo jih vzorčili iz vzrejne čebelje družine in kontrolne družine s čebeljo matico. Premer acinusov je pri delavkah v starosti 1 do 30 dni iz vzrejne družine znašal 109,2 do 180,9 µm, pri delavkah iste starosti iz kontrolne družine pa od 100,8 do 158,2 µm. Ugotovili smo, da so imele čebele krmilke iz vzrejne družine (graditeljice celic), stare od 15 do 27 dni, statistično značilno večji premer acinusov ($p<0.0001$), kot smo ga izmerili pri delavkah iste starosti iz kontrolne skupine. Opisali smo morfološke in histološke značilnosti krmilnih žlez pri krmilkah v starosti od 1 do 27 dni in ugotovili, da je bilo izločanje pri delavkah, ki so krmile zalego, podaljšano v primerjavi z delavkami iz kontrolne skupine. Nadalje smo opisali krmilne žleze pri bubah delavk pred izleganjem in pri zimskih čebelah iz kontrolne družine. Rezultati so pokazali, da so krmilne žleze pri bubi sestavljene iz skupkov neenako oblikovanih acinusov. Celična citoplazma ni strukturirana in je homogena, jedra so gosta in ovalne oblike. Pri zimskih čebelah smo našli hipertrofirane krmilne žleze, ki so vsebovale številne vezikle, v katerih se je nalagal izloček. Acinusi zimskih čebel so večji, goste strukture in so mlečno bele barve. V prispevku smo opisali tudi fiziološko funkcijo krmilnih žlez in s starostjo povezana opravila delavk krmilk.

Ključne besede: premer acinusov; starost; morfologija; krmilka; zimska čebela; buba delavke

Slov Vet Res 2015; 52 (2): 75-85
UDC 577.352:546.26:612.111:636.7

Original Scientific Article

EFFECT OF CARBON BLACK NANOMATERIAL ON CANINE ERYTHROCYTE AND PLATELET SHAPE

Judita Lea Krek[1], Metka Šimundić[3], Mitja Drab[1], Manca Pajnič[1], Vid Šuštar[4], Roman Štukelj[1], Damjana Drobne[2], Veronika Kralj-Iglič[1]

[1]Laboratory of Clinical Biophysics, Faculty of Health Sciences, University of Ljubljana, Zdravstvena pot 5; [2]Group of Nanobiology and Nanotoxicology, Department of Biology, University of Ljubljana, Večna pot 111; [3]Prva Clinics for Small Animals, Gorkičeva 6, 1000 Ljubljana, Slovenija, [4]Lymphocyte Cytoskeleton Group, Department of Pathology, University of Turku, Medical Faculty, Tykistökatu 6B, FIN-20520 Turku, Finland

*Corresponding author, E-mail: veronika.kralj-iglic@fe.uni-lj.si

Summary: The effect of carbon black agglomerated nanomaterial on biophysical properties of canine red blood cell and platelet membranes that are reflected in changes of cell shape, was studied. Samples of canine blood diluted with citrated and phosphate buffered saline were incubated with carbon black nanomaterial and observed by scanning electron microscope and optical microscope. Interaction of agglomerated nanomaterial with erythrocyte membrane was observed. The relative abundance of different erythrocyte shape types (discocytes, echinocytes, spherically shaped erythrocytes) was determined on populations of cells, in suspensions with added carbon black nanomaterial and in control suspensions. Ensembles composed of representative images of cell populations were assessed by statistical methods. A two dimensional mathematical model of the erythrocyte shape was constructed to illustrate and explain erythrocyte swelling of intially discocytic/echinocytic shape to the final spherical shape, which preceeds membrane rupture. Micrometre-sized agglomerates were formed in the blood and interacted with erythrocyte membrane without evidently disturbing local membrane curvature or global cell shape. Incubation of blood with citrated and phosphate buffered saline caused a time dependent decrease of the number of intact erythrocytes in samples that was ascribed to a disintegration of erythrocyte membranes. The presence of carbon black nanomaterial in the samples suppressed this effect. Relative proportions of cell shape types remained largely unchanged within 24 hours of observation of the test and the control sample. The observed effects of carbon black nanomaterial can be described as originating from osmosis. Incubation of canine platelets with carbon black nanomaterial within 24 hours preserved the disc-like shape that is characteristic for resting platelets. It was concluded that carbon black nanomaterial interacts with membranes of blood cells but does not have a direct effect on the local or global membrane shape. However, large size of carbon black agglomerates, that can be formed in blood plasma could present mechanical obstacles in the cardiovascular system.

Key words: carbon black; nanoparticles; erythrocyte shape; osmosis; nanomaterial safety; nanotoxicology; alternatives to laboratory / experimental animals

Introduction

Environmental pollution is a subject of increasing interest due to its potentially harmful effect on the health of human (1-4) and animals (5-8). Carbon black (CB) is produced by the incomplete combustion of petroleum products, such as in traffic. When inhaled, small enough particles of CB can enter the circulation and in this way also reach the tissue cells. The adverse effects of CB on health were observed (9-11) while for scientific and medical purposes, the possible mechanisms were studied in vitro (12-15) and in vivo (15). Studies on experimental animals have shown changes in development, in the immune response and in gene expression (15), however, mechanisms underlying harmful effects of CB

Received: 25 July 2014
Accepted for publication: 6 February 2015

on human and animals are yet obscure. Some authors report that the effects of nanomaterial depends primarily on the shape and size of nanoparticles, rather than on their composition (16). This suggests, that non-specific biophysical mechanisms are relevant to describe the effect of nanoparticles on cells and should therefore be included in analyses of the effects of nanomaterial on cells and organisms.

By choosing an appropriate experimental system, the relevant conditions can be achieved and higher standard ethical principles applied in human and in animals (17). Studying basic biophysical mechanisms including the interaction of the test compound with blood cells requires a minimally invasive procedure (taking a small volume of blood) and no material that impairs health and well being of animals. In this work, the in vitro effect of CB on biophysical properties of canine erythrocyte and platelet membranes were considered. As mature mammalian erythrocytes have no internal structure, exogenously added particles that interact with the membrane can cause changes in its properties which is revealed in the change of cell shape (13,21-26). The equilibrium shape of erythrocyte is determined solely by the minimum of the membrane free energy (18,19). Shape changes and mediated interactions are relevant also for platelets, especially since they indicate a propensity of platelets for disturbances in blood clotting that may lead to thromboembolisms (20). It is the aim of this work to consider the effect of carbon black nanomaterial on biophysical properties of biological membranes, that can be deduced from the observed shape changes of erythrocytes and platelets.

Material and methods

Carbon black nanomaterial and suspensions

Nanopowder of CB was purchased from PlasmaChem GmbH (Berlin, Germany) with the average size of primary particles of 13 nm. For experiments with diluted blood samples, washed erythrocytes or platelet rich plasma, stock suspensions of 5 mg/mL CB were prepared in citrated and phosphate buffered saline (PBS): 137 mM NaCl, 2.7 mM KCl, 10 mM $Na_2HPO_4x2H_2O$, 2 mM KH_2PO_4, 10.9 mM $Na_3C_6H_5O_7$. The final concentration of CB in the sample was 1 mg/ml (26).

Blood sampling

The procedures conformed to the European Union's legislation and were in accordance with guidelines set by the Committee for Research and Ethical Issues of IASP. Sampling was performed according to the Declaration of Helsinki and a written informed consent to take blood was given by the animal owners. Blood was taken from two healthy middle-sized pet dogs for which the sample volume represented about 1% of total blood volume. The study was approved by the National Ethics Committee, No 117/02/10. No adverse effects on animals' health due to sampling were observed.

For SEM imaging 10 mL of blood was collected from two healthy dogs (female, 2 years, 13 kg and male, 12 years, 11 kg) into 2.7 mL tubes containing 270 μL trisodium citrate at a concentration 0.109 mol/L (BD Vacutainers, Becton Dickinson, CA). Blood was collected by vein puncture by using a 21-gauge needle (length 70 mm, inner radius 0.4 mm) (Microlance, Becton Dickinson, NJ, USA). Blood was pulled by a syringe.

For direct observation under the optical microscope, 1 mL of blood was collected from a healthy dog (female, 6 years) as described above into a plastic tube without anticoagulant. A drop of blood was taken from the collecting tube immediately after the sampling with a pipette, inserted into an Eppendorf tube previously filled with 1 mL of PBS and gently mixed by turning the sample upside down.

Preparation of blood cells for electron microscopy

Blood was processed within 1 hour from sampling according to previously used protocols (27,13). Blood was centrifuged in a Centric 400R centrifuge (Domel d.o.o., Železniki, Slovenia) at 50 g and 37°C for 15 minutes to separate erythrocytes from platelet rich plasma. Erythrocytes were repeatedly washed with PBS citrate by centrifugation at 1550 g and 37°C for 10 minutes. Washed erythrocytes or platelet rich plasma were aliquoted into equal parts (50 μL in case of erythrocytes and 200 μL in case of platelet rich

plasma). CB suspended in PBS-citrate (or PBS-citrate alone for control) was added to aliquotes in v/v ratio of 2:1 in case of erythrocytes and 3:1 in case of platelet rich plasma, 3 and 2 units corresponding to erythrocytes and platelet rich plasma, respectively. After incubation for 1 hour, the samples were fixed in 0.1% glutaraldehyde, incubated for another hour at room temperature and centrifuged at 1550 g and 37°C for 10 minutes to allow erythrocytes to weakly agglomerate (in order to keep them grouped in pellet for further processing). Supernatant was exchanged for PBS-citrate, samples were resuspended and fixed in 2% glutaraldehyde for an hour at room temperature.

Scanning electron microscopy of blood cells

Fixed samples were washed by exchanging supernatant with citrated PBS and incubated for 20 minutes at room temperature. This procedure was repeated 4 times while the last incubation was performed over night at 8 °C. Samples were then post-fixed for 60 min at 22 °C in 1% OsO_4 dissolved in 0.9% NaCl, dehydrated in a graded series of acetone/water (50%-100%, v/v), critical-point dried, gold-sputtered, and examined using a LEO Gemini 1530 (LEO, Oberkochen, Germany) scanning electron microscope.

Population study of CB effect on erythrocyte shape

PBS-diluted blood samples incubated with the test or control solution were observed under the Leitz Aristoplan (Leitz, Wetzlar, Germany) optical microscope connected to the Watec (Model: 902DM3S), Watec Inc., New York, USA, camera and Pinnacle Studio HD, Version 15.0.0.7593 framegraber and software, Avid Technology Inc., USA. The magnification of the objective was 63 x. The sample was diluted to obtain a density of blood cells composing a monolayer with at least 20 cells on the average in a frame. The test sample was composed of 175 mL of diluted blood and 25 mL of suspended nanomaterial while the control sample was composed of 175 mL of diluted blood and 25 mL of PBS. An observation chamber 1.5 x 1 cm^2 was created on the glass by using silicon grease. 40 μL of the test suspension was placed in the observation chamber and closed by gently pressing the cover glass. Care was taken not to leave voids in the grease boundary in order to prevent evaporation of liquid from the observation chamber. For quantitative analysis of the effect of CB NPs on blood cell membranes, at least 50 frames were randomly imaged over the sample. The images were taken 1 hour, 3 hours and 24 hours after placing the samples into the observation chambers. Regions close to the silicon grease were avoided. During the incubation the samples were kept at the room temperature.

Image analysis of erythrocyte populations

Diluted blood samples contained mostly erythrocytes and singular leukocytes. Leukocytes were not considered. For each sample an ensemble of pictures was created in which we were able to clearly distinguish different possible cell shape types (discocytes, echinocytes, stomatocytes and spherical shapes). The number of intact cells of each shape type was determined in each picture. It was assumed that the pictures were representative for the sample and that the number of cells of each shape type fluctuated around the corresponding average value. The average values of the percent of discocytes, echinocytes, stomatocytes and spherical cells were calculated. 5087 erythrocytes were included in the analysis.

Statistical analysis

The two tailed paired t-test with equal variance to compare the average values was used. Differences with $p<0.05$ were considered statistically significant. Power analysis was performed to validate the size of the samples. Power larger than 0.85 at $\alpha<0.05$ indicated the sample of a proper size. Microsoft Excell software (Microsoft® Office Excel® 2007 SP3) and Power & Sample Size Calculator were used for calculation.

Theoretical model of the cell shape

A two dimensional model of the cell without internal structure was constructed to illustrate the observed shape changes. In the model, the cell membrane was represented by a closed curve with bending but no stretching properties. The curve was described by using polar coordinates (ρ,θ) (Figure 1).

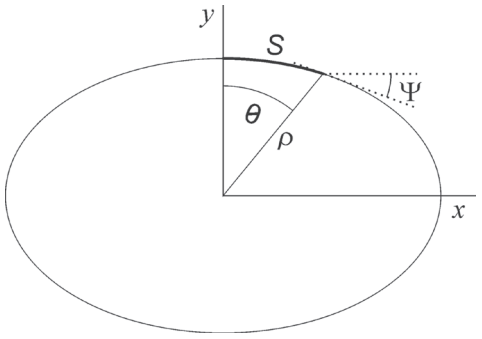

Figure 1: Parametrization of the shape

For convenience, the curve was parametrized by introducing the arclength S and the angle between the tangent to the curve and the x-axis Ψ (Figure 1). The equations of differential geometry give the curvature in terms of the parameters S and Ψ,

$$\dot{\Psi} = C(S), \tag{1}$$

where the dot denotes a derivative with respect to S, $\dot{\Psi} = \mathrm{d}\Psi/\mathrm{d}S$. The bending energy of the curve is given by

$$W_\mathrm{b} = \frac{k_\mathrm{c}}{2}\int_0^L \mathrm{d}S\,(C - C_0)^2, \tag{2}$$

where L is the perimeter of the curve k_c is the two dimensional elastic constant, $\mathrm{d}S$ is the arclength element and C_0 is the spontaneous curvature of the membrane. The spontaneous curvature does not enter the shape equations due to the Gauss-Bonnet theorem. The free energy of the two dimensional erythrocyte is composed of the elastic bending energy and the enthalpic term PA:

$$F = W_\mathrm{b} + PA, \tag{3}$$

where A is the enclosed area and P is the two-dimensional pressure.

Dimensionless quantities are introduced. We define R as a radius of the circle with fixed membrane circumference

$$R = \frac{L}{2\pi}. \tag{4}$$

Dimensionless arclength s, dimensionless curvature c and dimensionless pressure p take on the respective forms

$$s = \frac{S}{R}, \qquad c = CR, \qquad p = \frac{PR^3}{k_c}. \tag{5}$$

The enclosed area is normalized with respect to the maximal possible enclosed area A_max

$$a = \frac{A}{A_\mathrm{max}} \tag{6}$$

$$A_\mathrm{max} = \pi R^2$$

and the membrane free energy is normalized with respect to the bending energy of a circle with

$C_0 = 0$, ($W_{\mathrm{b,\,circle}} = k_\mathrm{c}\,\pi/R$):

$$w_b = \frac{1}{2\pi}\int_0^{2\pi} c^2\,\mathrm{d}s. \tag{7}$$

Minimization of the dimensionless membrane free energy was performed by variation of the free energy $\delta F = 0$. The constraints requiring fixed curve perimeter

$$1 = \int_0^1 \mathrm{d}s \tag{8}$$

and fixed enclosed area

$$a = \int_0^1 x(s)\sin\Psi(s)\,\mathrm{d}s \tag{9}$$

were taken into account.

The dimensionless area can take on values within the interval $a \in [0,1]$, with 1 corresponding to a circle. The variational problem was solved using Euler-Lagrange formalism, which yielded four coupled differential equations

$$\ddot{\Psi}(s) - px(s)\cos\Psi(s) - \kappa(s)\sin\Psi(s) = 0,$$

$$\dot{x}(s) - \cos\Psi(s) = 0, \quad \dot{y}(s) + \sin\Psi(s) = 0,$$

$$\dot{\kappa}(s) - p\sin\Psi(s) = 0, \tag{10}$$

where $x(s)$ and $y(s)$ denote the plane coordinates and $\kappa(s)$ is a local Lagrange multiplier. The equations were solved numerically by the shooting method. Mathematica, Wolfram Reserch, Inc. (version 9.0.1.0, Champaign, U.S.A.) was used for calculation. Some results were further rendered by Surface Evolver, an open-source software (version 2.70, Susquehanna, U.S.A.), available at http://www.susqu.edu/brakke/evolver/evolver.html.

Results

Figure 2 shows the effect of CB on washed erythrocytes (A) and platelets (B) as observed by the scanning electron microscope (SEM). Erythrocytes and platelets were incubated with CB nanomaterial for 1 hour. Most of the cells in Figure 2A reveal discocytic shape (short arrow). Deposited material can be seen on the erythrocyte surface that could correspond to CB agglomerates (long arrow). Agglomerates adhered to the erythrocyte surface but did not cause distortion of local membrane curvature. Incubation of platelets with CB nanomaterial preserved the disc-like shape chacteristic for resting platelets (Figure 2B).

The effect of CB nanomaterial on populations of erythrocytes in PBS-diluted blood samples is shown in Figures 3 and 4. Discocytes (Figure 3B, black triangle), echinocytes (Figure 3B, white arrow), spherically shaped cells (Figure 3C, white arrow) and ghosts (Figure 3C, black/white striped arrows) can be distinguished. The contrast in Figure 3C was enhanced to make the ghosts visible.

The number of cells in the test sample and in the control sample diminished with time (Figure 3, Figure 4A), the effect being stronger in control. The differences between the average values of the number of erythrocytes in the frame after 1 hour, 3 hours and 24 hours were statistically significant with sufficient power ($p<10^{-4}$, $P(\alpha=p) > 0.95$). After 1 hour, the control sample contained a higher proportion of echinocytes than the test sample (Figure 4B). No trend for an increase or a decrease of the average proportions of the respective cell types in the test and in the control with time (Figure 4 B,C,D) was observed.

These results indicate that the osmotic effects took place during the observed transformations. As these effects took place also in the control sample, a possible explanation would be that the osmotically active particles were removed from the outer solution by adhering to the glass of the observation chamber and/or by interacting with each other. To attain the Donnan equilibrium, water entered the cells and induced a shape transformation towards the sphere. As the cell membrane poorly tolerates stretching, the continuation of this process caused membrane disintegration and ghost formation. The process took place gradually with time. In the test sample, the added CB nanomaterial changed the osmolarity of the solution in a way to suppress the above process. Nanoparticles increased the osmolarity of the solution by intervening with the adhesion of solutes to the glass and/or with their mutual interaction. Osmotic swelling of cells was therefore decelerated with respect to the control sample.

The theoretically calculated sequence illustrates the suggested mechanism. Figure 5 shows two sequences of calculated two dimensional shapes simulating erythrocyte swelling, starting from a discocyte (a) and an echinocyte (d). Swelling was simulated by increasing the area enclosed by the curve. Initial echinocytic shape had higher energy than the discocytic shape, but increasing the enclosed area diminished the energies and led both sequences to the final circular shape. Thus, the two sequences presented in Figure 5 correspond to two branches in the phase diagram trajectories.

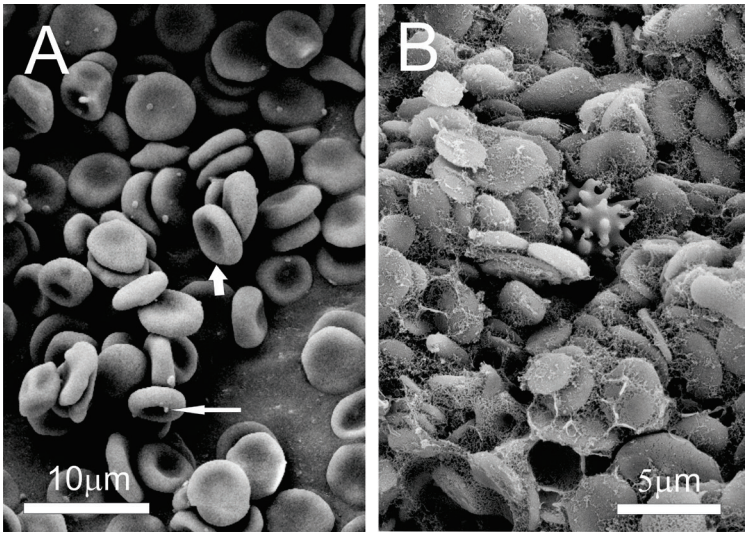

Figure 2: Scanning electron microscope (SEM) images of canine erythrocytes (A) and platelets (B) incubated with carbon black for 1 hour. Carbon black agglomerates adhered to the erythrocyte surface (long arrow) but the normal discoid shape of erythrocytes was preserved (short arrow). Platelets incubated with carbon black for 1 hour retained disc-like shape

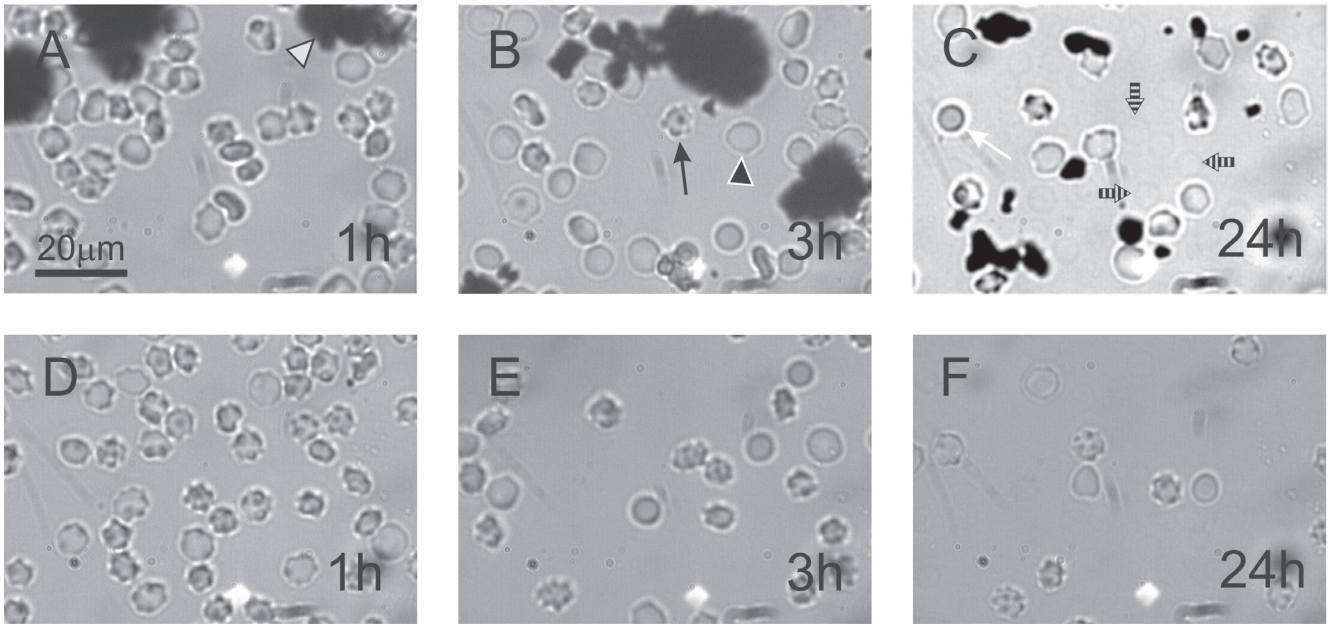

Figure 3: Optical microscope images of populations of PBS-diluted canine blood incubated with carbon black (A-C) after 1 hour, 3 hours and 24 hours, respectively and control samples of PBS-diluted canine blood (D-F) after 1 hour, 3 hours and 24 hours, respectively. Characteristic shapes of erythrocytes: discocytes (B, black triangle), echinocytes (B, black arrow), spherically shaped cells (C, white arrow) and ghosts (C, black/white striped arrows) can be distinguished. White triangle points to a large carbon black aggolmerate (panel A). Contrast in panel C was enhanced to make the ghosts visible

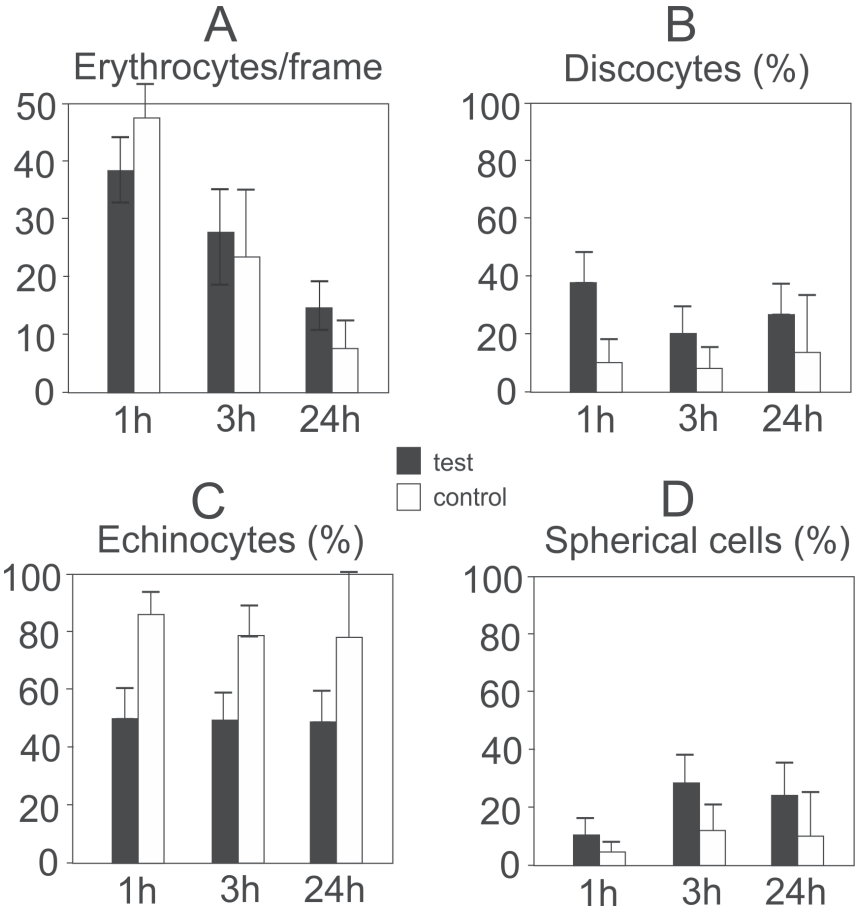

Figure 4: Abundance of erythrocytes with different shape types in the diluted canine blood. A: time dependence of the number of erythrocytes in the test sample and in the control sample, B: portion of the discocytes in the samples, C: portion of the echinocytes in the samples and D: portion of the spherically shaped cells in the samples. Bars denote standard deviations

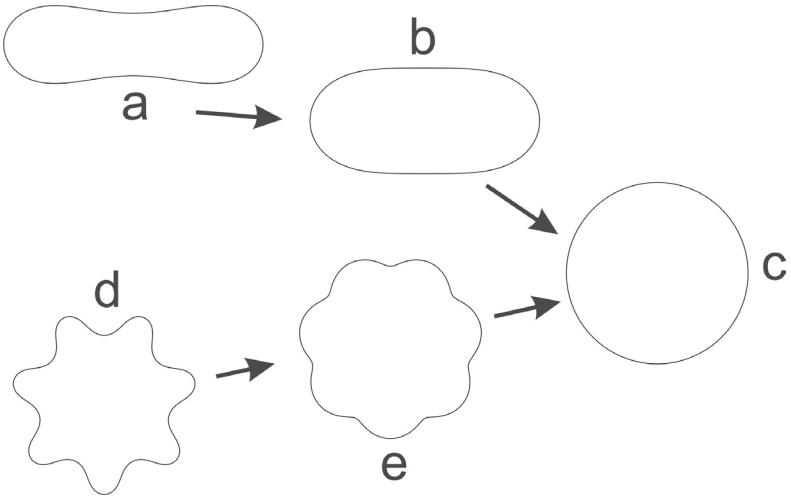

Figure 5: Theoretical description of the osmotic swelling of an erythrocyte starting from a discocyte (a-b-c) and an echinocyte (d-e-c). The shapes were calculated by a two dimensional model based on the minimization of the free energy of the curve at a given enclosed area. The swelling is simulated by an increase of the enclosed area a: 0.57 (shape a), 0.82 (shape b), 1 (shape c), 0.6 (shape d), 0.85 (shape e)

Discussion

In this work, the effect of carbon black nanoparticles on biophysical properties that are revealed in changes of the shape of erythrocytes and platelets was considered. In erythrocytes, haemolytic effects of some types of nanoparticles were reported in the literature (16), where it was suggested that these effects of nanoparticles are due to the shape and size and not the composition of the NPs (16). Toxicity of carbon compounds was found to depend on configuration: nanotubes and quartz were much more toxic than carbon black (28). These effects cannot be explained by the chemical reactions but are related to biophysical mechanisms that were addressed in this work. Namely, shape changes induced by formation of inclusions in membranes lead to membrane budding, vesiculation and finally disintegration.

However, other effects ascribed to nanoparticles were reported in the literature. Production of reactive oxygen species (29), procoagulant activity (30), genotoxicity (31), and effects of biodistribution within the body (32) were reported in leukocytes. Carbon black nanoparticles were found to induce reactive oxygen species-mediated inflammatory effects in bronchial epithelial cell line; the effect correlated with the concentration of nanoparticles and the structure of their surface (33). Furthermore, nanoparticles were found to interact with plasma proteins causing changes in conformation, activation, and inhibition of plasma proteins, exposure of epitopes and changes in physicochemical properties of nanoparticles such as their ability to agglomerate or adsorb proteins (34-35), which influences the coagulation system (36). These effects may depend on time of incubation and amount of nanomaterial (34-35).

We found that CB NPs agglomerated in citrated and phosphate buffered saline and in platelet rich plasma. As regards the biophysical properties that affect the cell shape, no deleterious effects of CB on canine erythrocyte and platelet membranes were observed. Scanning electron micrographs showed that larger CB agglomerates adhered to the erythrocyte membrane but did not distort the local membrane curvature nor the global cell shape (Figure 2A). A decrease of the number of intact erythrocytes in samples in the time interval of 24 hours was observed in the suspensions of PBS-diluted blood (Figure 4A), however, this effect was present also in the control sample (Figure 4A). The number of cells diminished at the expense of the number of ghosts which are poorly visible in the images unless the image is processed (as in Figure 3C). Moreover, spherically shaped cells are present in the samples (Figure 3) indicating that erythrocyte underwent swelling prior to the erythrocyte-ghost transformation. Although the initial number of cells was higher in the control sample (Figure 4A), it decreased more rapidly with time than the number of cells in the test sample, so after 24 hours the number of cells with preserved membrane was considerably and statistically significantly higher in the test sample ($p<10^{-4}$, $P(\alpha=p) > 0.95$).

The theoretical sequences in some aspect illustrate the suggested transformations to sphere derived from the experimental observations, however, the two-dimensional model cannot

describe all the properties of the intermediate shapes.Thus, the extensions of the two dimensional shapes (Figure 5) do not refer to the extensions of the contours of imaged erythrocytes (Figure 3) as the cell volume requires an extension also in the direction perpendicular to the image plane. This is in contrast with the calculated sequence (Figure 5) where the enclosed area increases. It should be kept in mind that the enclosed area of the shapes in Figure 5 represents the cell volume of real cells which increases in osmotic swelling.

In three dimensional models, minimization of the bending energy of laterally isotropic membrane (37) (which is analogous to the expression used in this work) cannot explain the stable shape of the echinocyte but including the shear energy of the membrane skeleton provides a possible explanation (38,39). By using a geometrical ansatz for the shape of the spicules and distributing the spicules over the spherical surface it was found that in the echinocyte – spherical cell transformation the echinocyte spicules become more numerous and thinner when the transformation is driven by an increase of the difference between the outer and the inner membrane layer area (38). A more refined model where the shape of the spicules was determined by a rigorous solution of the variational problem confirmed these results (39). Previous models did not present a rigorous solution to the variational problem for the entire cell which is an advantage of the two dimensional model presented in this work.

Previous theoretical work regarding shape transformation of echinocyte into spherical cell considered mostly processes driven by the change of the difference between the outer and the inner membrane layer areas (40-43). This mechanism takes place if exogeneously added molecules intercalate preferentially in the outer membrane layer (41-43) or due to the conformational change of membrane proteins (44). These results cannot be directly applied to the features considered in our work where the presented two dimesional model provided an illustration of a possible trajectory of shapes in osmotic swelling of initially mildly undulated echinocytes.

CB nanomaterial preserved the disc-like shape of resting platelets (Figure 2B). In contrast, the effect of ZnO nanomaterial was previously found to cause shape transformation of platelets (13). ZnO-treated platelets were considerably rounded and presented tubular protrusions characteristic for activated platelets while CB treated platelets did not exhibit such features. Furthermore, it was previously reported that CB nanoparticles had no effect on the platelet aggregation (26). On the other hand, certain carbon particles stimulated platelet aggregation and accelerated the rate of vascular thrombosis in rat (45).

This study indicates that carbon black nanomaterial may affect blood cells of animal and human indirectly through osmotic effects which were in this study found the most prominent. However, the test sample after 1 hour also contained considerably higher proportion of discocytes than the control sample (Figure 4B) which did not necessary derive from osmotic effects. In order to answer the question whether CB nanomaterial exerts harmful effects on blood cell membranes more refined studies are necessary, including the effect of the integrity of the membrane skeleton (46-48), lateral inhomogeneities of the membrane (49,50), complex interactions between the molecules in the solution (51-53) and microexovesiculation (54) on the cells and their environment.

Conclusions

The effect of CB nanomaterial on the canine erythrocyte membranes was observed. CB agglomerates adhered to the erythrocytes but by that did not cause local or global shape change. Observed hemolysis in the in vitro control samples was explained by the osmotic effects. CB nanomaterial suppressed this hemolytic effect which can be explained by its direct and indirect effect on the osmolarity of the solution. Activation of platelets after 1 hour of incubation with CB nanomaterial was not observed. No harmful direct in vitro effect of CB nanomaterial on the erythrocyte and platelet membrane shapes was found on the level of cell populations.

Acknowledgements

Authors acknowledge support from Slovenian Research Agency fund J1-4109, J3-4108 and P3-0388.

1. Yeates DB, Mauderly JL. Inhaled environmental/occupation irritants and allergens: mechanisms of cardiovascular and systemic responses: introduction. Environ Health Persp 2001; 109: 479–81.

2. Oberdorster G, Oberdorster E, Oberdorster J. Nanotoxicology: an emerging discipline evolving from studies of ultrafine particles. Environ Health Persp 2005; 113: 823–39.

3. Colvin V. The potential environmental impact of engineered nanomaterials. Nat Biotechnol 2003; 13: 1166–70.

4. Vermylen J, Nemmar A, Nemery B, Hoylaerts FM. Ambient air pollution and acute myocardial infarction. J Thromb Haemost 2005; 3 :1955–61.

5. Backer LC, Grindem CB, Corbett WT, Cullins L, Hunter JL. Pet dogs as sentinels for environmental contamination. Sci Total Environ 2001; 274: 161–9.

6. Goodarzi M, Azizi S, Koupaei MJ, Moshkelani S. Pathologic findings of anthraco-silicosis in the lungs of one humped camels (*Camelus dromedarius*) and its role in the occurrence of pneumonia. Kafkas Univ Vet Fak Derg 2014; 20: 171–6.

7. Beytut E. Anthracosis in the lungs and associated lymph nodes in sheep and its potential role in the occurrence of pneumonia. Small Ruminant Res 2002; 46:15–21.

8. Curi NHD, Brait CHH, Antoniosi NR, Talamoni SA. Heavy metals in hair of wild canids from the Brazilian Cerrado. Biol Trace Elem Res 2012; 147: 97–102.

9. Reijnders L. Human health hazards of persistent inorganic and carbon nanoparticles. J Mater Sci 2012; 47: 5061–73.

10. Gardiner K, van Tongeren, Harrington M. Respiratory health effects from exposure to carbon black: results of the phase 2 and 3 cross sectional studies in the European carbon black manufacturing industry. Occup Environ Med 2001; 58: 496–503.

11. Ling MP, Chio CP, Chou WC, et al. Assessing the potential exposure risk and control for airborne titanium dioxide and carbon black nanoparticles in the workplace. Environ Sci Pollut R 2011; 18: 877–89.

12. Vattanasit U, Navasumrit P, Khadka MB, et al. Oxidative DNA damage and inflammatory responses in cultured human cells and humans exposed to traffic – related particles. Int J Hyg Environ Health 2014; 217: 23–33.

13. Šimundić M, Drašler B, Šuštar V, et al. Effect of engineered TiO2 and ZnO nanoparticles on erythrocytes, platelet-rich plasma and giant unilamelar phospholipid vesicles. BMC Vet Res 2013; 9: e7 (13 p) http://www.biomedcentral.com/content/pdf/1746-6148-9-7.pdf

14. Ucciferi N, Collnot EM, Gaiser BK, et al. In vitro toxicological screening of nanoparticles on primary human endothelial cells and the role of flow in odulating cell response. Nanotoxicology 2013; 8: 697–708.

15. Ema M, Naya M, Horimoto M, Kato H. Developmental toxicity of diesel exhaust: a review of studies in experimental animals. Reprod Toxicol 2013; 42: 1–17.

16. Mocan T. Hemolysis as expression of nanoparticles-induced cytotoxicity in red blood cells. Biotechnol Mol Biol Nanomed BMBN 2013; 1(1): 7–12.

17. Van Vliet E. Current standing and future prospects for the technologies proposed to transform toxicity testing in the 21st century. ALTEX 2011; 28: 17–44.

18. Canham PB. The minimum energy of bending as a possible explanation of the biconcave shape of the human red blood cell. J Theor Biol 1970; 26: 61–81.

19. Seifert U. Configurations of fluid membranes and vesicles. Adv Phys 1997; 46:13–137.

20. Gorbet MB, Sefton MV. Biomaterial-associated thrombosis: roles of coagulation factors, complement, platelets and leukocytes-rewiev. Biomaterials 2004; 25: 5681–703.

21. Suwalsky M, Villena F, Norris B, et al. Structural effects of titanium citrate on the human erythrocyte membrane. J Inorg Biochem 2005; 99:764–70.

22. Suwalsky M, Novoa V, Villena F, et al. Structural effects of Zn (2+) on cell membranes and molecular models. J Inorg Biochem 2009; 103:797–804.

23. Suwalsky M, Hernandez P. Aluminum enhances the toxic effects of amyloid beta-peptide on cell membranes and a molecular model. Monatsh Chem 2011; 142: 431–7.

24. Rothen - Rutishauser BM, Schurch S, Haenni B, Kapp N, Gehr P. Interaction of fine particles and nanoparticles with red blood cells visualized with advanced microscopic techniques. Environ Sci Technol 2006; 40: 4353–9.

25. Solomon A, Smyth E, Mitha N, et al. Induction of platelet aggregation after a direct physical interaction with diesel exhaust particles. J

Thromb Heamost 2013; 11: 325–34.

26. Drašler B, Drobne D, Novak S, et al. Effects of magnetic cobalt ferrite nanoparticles on biological and artificial lipid membranes. Int J Nanomed 2014; 9: 1559–81.

27. Šuštar V, Bedina - Zavec A, Štukelj R, et al. Nanoparticles isolated from blood: a reflection of vesiculability of blood cells during the isolation process. Int J Nanomed 2011;6: 2737–48.

28. Tsuji JS, Maynard AD, Howard, et al. Research strategies for safety evaluation of nanomaterials. Part IV: Risk assessment of nanoparticles. Toxicol Sci 2005; 89: 42–50.

29. Piryazev AP, Azizova OA, Aseichev AV, Dudnik LB, Sergienko VI. Effect of gold nanoparticles on production of reactive oxygen species by human peripheral blood leukocytes stimulated with opsonized zymosan. Bull Exp Biol Med 2013; 156: 101–3.

30. Dobrovolskaia MA, Patri AK, Potter TM, Rodriguez JC, Hall JB, McNeil SE.Dendrimer-induced leukocyte procoagulant activity depends on particle size and surface charge. Nanomedicine 2012; *7*: 245–56.

31. Colognato R, Bonelli A, Ponti J, Farina M, Bergaaschi E, Sabbioni E, Migliore L. Comparative genotoxicity of cobalt nanoparticles and ions on human peripheral leukocytes in vitro. Mutagenesis 2008; 23: 377–82.

32. Aggarwal P, Hall JB, McLeland CB, Dobrovolskaia MA, McNeil SE. Nanoparticle interaction with plasma proteins as it relates to particle biodistribution, biocompatibility and therapeutic efficacy. Adv Drug Deliv Rev 2009; 61: 428–37.

33. Hussain S, Boland S, Baeza-Squiban A, et al. Oxidative stress and proinflammatory effects of carbon black and titanium dioxide nanoparticles: role of particle surface area and internalized amount. Toxicology 2009; 260: 142–9.

34. Tsai DH, DelRio FW, Keene AM, et al. Adsorption and conformation of serum albumin protein on gold nanoparticles investigated using dimensional measurements and in situ spectroscopic methods. Langmuir 2011; 27: 2464–77.

35. Izak-Nau E, Voetz M, Eiden S, Duschl A, Puntes VF. Altered characteristics of silica nanoparticles in bovine and human serum: the importance of nanomaterial characterization prior to its toxicological evaluation. Part Fibre Toxicol 2013; 10: e56 (12 p.) http://www.particleandfibretoxicology.com/content/pdf/1743-8977-10-56.pdf

36. Ilinskaya AN, Dobrovolskaia MA. Nanoparticles and the blood coagulation system. Part II: safety concerns. Nanomedicine (Lond) 2013; 8: 969–81.

37. Deuling HJ, Helfrich W. The curvature elasticity of fluid membranes: a catalogue of vesicle shapes. J Phys 1976; 37: 1335–45.

38. Iglič A. A possible mechanism determining the stability of spiculated red blood cells. J Biomech 1997; 30: 35–40.

39. Mukhopadhyay R, Lim HWG, Wortis M. Echinocyte shapes: bending, stretching, and shear determine spicule shape and spacing. Biophys J 2002; 82:1756–72.

40. Sheetz MP, Singer SJ. Biological membranes as bilayer couples: a molecular mechanism of drug-erythrocyte interactions. Proc Natl Acad Sci 1974; 71: 4457–4461.

41. Iglič A, Kralj - Iglič V, Hägerstrand H. Amphiphile induced echinocyte-spheroechinocyte red blood cell shape transformation. Eur Biophys J 1998; 27: 335–9.

42. Iglič A, Kralj-Iglič V, Hägerstrand H. Stability of spiculated red blood cells induced by intercalation of amphiphiles in cell membrane. Med Biol Eng Comput 1998; 36: 251–5.

43. Iglič A, Hägerstand H. Amphiphile-induced spherical microexovesicle corresponds to an extreme local area difference between two monolayers of the membrane bilayer. Med Biol Eng Comp 1999; 37: 125–9.

44. Gimsa J, Ried C. Do band 3 protein conformational changes mediate shape changes of human erythrocytes? Mol Membr Biol 1995; 12: 247–54.

45. Radomski A, Jurasz P, Alonso - Escolano D, et al. Nanoparticle-induced platelet aggregation and vascular thrombosis. Br J Pharmacol 2005; 146: 882–93.

46. Bobrowska - Hägerstrand M, Hägerstrand H, Iglič A. Membrane skeleton and red blood cell vesiculation at low pH. Biochim Biophys Acta 1998; 1371: 123–8.

47. Hägerstrand H, Danieluk M, Bobrowska Hägerstrand M, et al. Influence of band 3 protein absence and skeletal structures on amphiphile- and Ca^{2+}-induced shape alterations in erythrocytes: a study with lamprey (*Lampetra fluviatilis*), trout (*Onchorhynchus mykiss*) and human erythrocytes. BBA Biomembranes 2000; 1466, 125–38.

48. Hianik T, Rybár P, Bernhardt I. Adiabatic compressibility of red blood cell membrane: in-

fluence of skeleton. Bioelectrochemistry 2000; 52: 197–201.

49. Mrówczyńska L, Salzer U, Iglič A, Hägerstrand H. Curvature factor and membrane solubilization, with particular reference to membrane rafts. Cell Biol Int 2011; 35: 991–5.

50. Mrówczyńska L, Salzer U, Perutková Š, Iglič A, Hägerstrand H. Echinophilic proteins stomatin, sorcin, and synexin locate outside ganglioside M1 (GM1) patches in the erythrocyte membrane. Biochem Biophys Res Commun 2010; 401: 396–400.

51. Mrówczyńska L, Bielawski J. The mechanism of bile salt-induced hemolysis. Cell Mol Biol Lett 2001; 6: 881–95.

52. Jasiewicz B, Mrówczyńska L, Malczewska-Jaskola K. Synthesis and haemolytic activity of novel salts made of nicotine alkaloids and bile avids. Bioorg Med Chem Lett 2014; 24: 1104–7.

53. Rudenko S V. Erythrocyte morphological states, phases, transitions and trajectories. Biochim Biophys Acta 2010; 1798: 1767–78.

54. Mrvar - Brečko A, Šuštar V, Janša V, et al. Isolated microvesicles from peripheral blood and body fluids as observed by scanning electron microscope. Blood Cells Mol Dis 2010; 44: 307–12.

VPLIV NANOMATERIALA ČRNEGA OGLJIKA NA OBLIKO PASJIH ERITROCITOV IN TROMBOCITOV

J. L. Krek, M. Šimundić, M. Drab, M. Pajnič, V. Šuštar, R. Štukelj, D. Drobne, V. Kralj-Iglič

Povzetek: Obravnavali smo vpliv aglomeriranega nanomateriala črnega ogljika na biofizikalne lastnosti membrane, ki se odražajo v spremembah celične oblike pasjih rdečih krvniček in trombocitov. Vzorce pasje krvi, razredčene s citriranim fosfatnim pufrom, smo inkubirali z nanomaterialom črnega ogljika in jih opazovali z vrstičnim elektronskim mikroskopom ter optičnim mikroskopom. Ugotovili smo, da aglomerati nanomateriala interagirajo z membrano eritrocita. Na populacijah smo opazovali število celic in deleže posameznih vrst celic glede na obliko (diskociti, ehinociti, kroglaste celice) v suspenziji z dodanim nanomaterialom črnega ogljika in v kontrolni suspenziji z dodanim citriranim fosfatnim pufrom. Kolektive, oblikovane iz reprezentativnih slik populacij celic, smo ocenili s statističnimi metodami. Za lažjo ponazoritev procesa osmotskega nabrekanja eritrocita iz začetne diskocitne ali ehinocitne v končno kroglasto obliko, ki ji sledi disintegracija membrane, smo izdelali dvodimenzionalni matematični model oblike eritrocita. V razredčeni krvi smo našli aglomerate nanomateriala črnega ogljika z največjo razsežnostjo v mikrometrskem območju. Aglomerati so interagirali z membrano eritrocita, ne da bi opazno spremenili lokalno ukrivljenost membrane in obliko celotne celice. Inkubacija krvi s citriranim fosfatnim pufrom je povzročila časovno odvisno zmanjševanje števila intaktnih eritrocitov v vzorcih, kar smo pripisali disintegraciji membrane eritrocita, pri čemer pa je dodan nanomaterial črnega ogljika deloval zaviralno. Relativni deleži posameznih vrst oblik so se v 24 urah v veliki meri ohranili. Opažene pojave smo lahko razložili z osmotskimi učinki. Inkubacija pasjih trombocitov z nanomaterialom črnega ogljika je v 24 urah ohranila diskasto obliko, ki je značilna za mirujoče trombocite. Ugotovili smo, da nanomaterial črnega ogljika interagira z membrano krvnih celic, vendar nima neposrednega učinka na lokalno in globalno obliko celice. Veliki aglomerati, ki nastanejo v krvni plazmi, pa bi lahko predstavljali mehanske ovire v krvnem obtoku.

Ključne besede: črni ogljik; nanodelci; oblika eritrocita; osmoza; varnost nanomaterialov; nanotoksikologija; alternativa laboratorijskim/poskusnim živalim

Slov Vet Res 2015; 52 (2): 87-95
UDC 577.2:615.214:616.092:599.323.452

Original Scientific Article

EFFICACY OF POTENTIAL ATYPICAL ANTIPSYCHOTIC LEK-8829 ON BEHAVIORAL EFFECTS IN RAT MODEL OF CATALEPSY AND INHIBITION OF AMPHETAMINE INDUCED PSYCHOMOTOR STIMULATION

Sanja Bogićević, Marko Živin*

Brain Research Laboratory, Institute of Pathophysiology, Faculty of Medicine, University of Ljubljana, Zaloška 4, 1000 Ljubljana, Marko Živin, University of Ljubljana, Slovenia.

*Corresponding author, E-mail: marko.zivin@mf.uni-lj.si

Summary: D2 antagonist drugs, such as haloperidol, are potent antipsychotic drugs but unfortunately also have a high propensity to cause unwanted extrapyramidal syndrome (EPS).
LEK-8829 is a dopamine D2 receptor antagonist with intrinsic activity at dopamine D1 receptors. Here we speculate that the intrinsic activity of LEK-8829 at dopamine D1 receptors may reduce its propensity to provoke EPS.
The experimental rats were thus behaviorally evaluated in sessions performed before and after the 21 day treatment period with haloperidol or LEK-8829, for the induction of catalepsy or for the inhibition of amphetamine-induced locomotor activity in the open field by the same dose of the respective drug as was used for 21 daily injections.
We found that after 21 day treatment with LEK-8829 or haloperidol, both drugs retained or even increased their potential for the induction of catalepsy. However, while LEK-8829 retained its efficacy for the inhibition of amphetamine-induced psychomotor stimulation, the efficacy of haloperidol was significantly diminished.
We conclude that LEK-8829 retains its antipsychotic efficacy during prolonged treatment and possess lower propensity for the induction of EPS as compared to typical neuroleptic haloperidol.

Key words: LEK-8829; dopamine D1 agonist; dopamine D2 antagonist; haloperidol; subchronic treatment

Introduction

Patients with schizophrenia exhibit positive, negative and cognitive symptoms that arise from an imbalance between the brain dopamine (DA) pathways mediating D2 and D1 receptor signaling (1, 2). Both hypo functioning and hyper functioning DA systems thus likely coexist in schizophrenia, albeit in different brain regions (4). Subcortical increase of DA, leading to hyperstimulation of D2 receptors, would give rise to the positive symptoms, while a concomitant cortical deficit of DA, leading to hypostimulation of D1 receptors, would give rise to the negative and cognitive symptoms. There is indeed robust evidence that DA hypofunction and altered D1 receptor signaling within the prefrontal cortex (PFC) play a central role in the induction of working memory deficits, suggesting that a reduced D1 receptor neurotransmission might cause cognitive impairments in schizophrenia (3).

Although the blockade of dopamine D2 receptors (4) is a prerequisite characteristic of all clinically effective antipsychotic drugs, the excessive blockade of dopamine D2 receptors within the basal

Received: 22 December 2014
Accepted for publication: 12 March 2015

ganglia often provokes unwanted extrpyramidal syndrome (EPS) (5,6,7,8,9), characterized by parkinsonism, akathisia, catalepsy, and, after long-term treatment, tardive diskinesia (7,8). A major disadvantage of typical antipsychotic (neuroleptic) drugs is their propensity for the production of EPS (8,9,10,11). LEK-8829 (9,10-didehydro-N-methyl-(2-propynyl)-6-methyl-8-aminomethylergoline) has been initially developed in order to be more effective and/or produce fewer side effects than typical antypsichotics drugs, such haloperidol. *In vitro* radioligand binding studies revealed that LEK-8829 possess low affinity for rat striatal 3H-SCH23390-labeled dopamine D1 binding sites and high affinity for striatal 3H-spiperone-labeled D2 and cortical 3H-ketanserin labeled serotonin-2 (5-HT2) sites. The ratio of pKi values 5-HT1/D2 was 1.11 (closer to that of clozapine than haloperidol) (12). Based on these experiments it has been concluded that the drug may be considered to have atypical antipsychotic potential (8). However, further behavioral, gene-expression and pharmacological studies in unilateral animal models of striatal dysfunction and cocaine self-administration have revealed that LEK-8829 also possess a considerable intrinsic activity at dopamine D1 receptors (13, 14). It has been therefore proposed that such pharmacological profile of antipsychotic drugs could alleviate both negative and positive symptoms of schizophrenia (15).

Catalepsy may be considered to represent an animal model for neuroleptic-induced parkinsonism in humans (16,17) and is often used for the evaluation of the liability of newly synthesized potentially antipsychotic drugs for the production of EPS (18). Amphetamine elevates dopamine release and in animal models reproduces the positive-like symptoms of schizophrenia. Inhibition of amphetamine-induced motor hyperactivity and behavioral disinhibition by antipsychotic drugs is used to evaluate their efficacy for the amelioration of positive symptoms (19, 20,21, 22).

In this study we propose that the likelihood for the development of EPS by the blockade of dopamine D2 receptors with LEK-8829 may be modified by its intrinsic activity at dopamine D1 receptors. We have therefore compared the effects of the prolonged treatment by LEK-8829 or by the reference neuroleptic drug, a dopamine receptor D2 antagonist haloperidol that does not possess intrinsic activity at dopamine D1 receptors, on their liability for the production of EPS and on their efficacy for the treatment of the positive symptoms of schizophrenia.

Materials and methods

Animals

A total adult 104 male Wistar rats (MEC, Ljubljana) with 270-300 g initial body weight were used in all experiments. The rats were housed four per cage under constant temperature and humidity, under 12 h light/dark cycles (on 8 am - off 8 pm). Food and water were continuously available *ad libitum* in home cages. The animals have been on adaptation in laboratory conditions for 14 days (before being used in experiments). All experiments were approved by Veterinary Administration of the Republic of Slovenia (34401-53/2012/7).

Drugs

LEK-8829 (Lek, Ljubljana, Slovenia), was calculated as the free base and dissolved in 0.9 % saline. Haloperidol (Haldol ampules, 5 mg/ml; Krka-Jenssen, Krka Novo Mesto, Slovenia) solution was diluted to appropriate concentration with 0.9% saline. LEK-8829 or haloperidol were injected subcutaneously (*s.c.*) in the neck region and administered dissolved in the volume of 2 ml/kg body weight, respectively. Amphetamine (RBI, Natick, MA, USA) was dissolved in 0.9% saline and injected 2 mg/kg and administered *s.c.*

Catalepsy

Catalepsy was performed by the method described by Krisch (12). It was assessed by the placement of the front limbs of the rats over a horizontal bar (11 cm above the floor). Catalepsy was scored every 20 min for 260 min. The scoring started 20 min after the *s.c.* injection of the test compounds (LEK-8829 or haloperidol). The score was assigned on the basis of the duration of the cataleptic posture (i.e. until one forepaw touched the floor or the hind legs left the floor to climb onto the bar as follows: score 1 - between 15 and 29 s; score 2 -between 30 and 59 s; and score 30 - 60 s or more.

Inhibition of amphetamine-induced locomotor activity

Locomotor activity in the open field was measured in individual boxes (60cm x 40cm). Rats were given *s.c.* injection of test compounds (LEK-8829 or haloperidol 2 mg/kg and 0.2 mg/kg, respectively) and were put in the open field. After20 min in the open field they were given an injection of amphetamine (2 mg/kg). Locomotor activity for individual rats was measured as distance moved in 120 min period using video tracking system for automation of behavioral experiments Noldus Ethovision Pro Version 3.0 (Noldus Information Technology, Wageningen, Netherlands).

Experiment 1

Seven groups of eight animals were used. All groups have been treated once daily for 21 days with drugs or 0.9% saline. The first group was treated with 0.9% saline. The second and the third group were treated with LEK-8829 (2 mg/kg, 0.2 mg/kg). The fourth and the fifth group were treated with haloperidol (2mg/kg, 0.2 mg/kg). In these five groups the catalepsy response was measured on day 1 and on day 21 of the experiment after injection with the same dose of the respective drug that was used for daily treatments. On all other days, the animals were put back into home cages immediately after drug injection.

The sixth group was treated with 0.9 % saline. The seventh group was treated with LEK-8829 (2 mg/kg). However, in these two groups the catalepsy response was evaluated on day 1 and on day 28 of the experiment so that between day 21 and day 28 the rats no received drug treatment.

Experiment 2

Six groups of eight animals were used. Animals have been treated once daily for 21 days. The first group was treated with 0.9 % saline. The second and the third group were treated with LEK-8829 (2 mg/kg, 0.2 mg/kg). The fourth group was treated with 0.9 % saline. The fifth and the sixth group were treated with haloperidol (2 mg/kg, 0.2 mg/kg). They were tested for the inhibition of amphetamine-induced locomotion with LEK-8829 (2 mg/kg, 0.2 mg/kg) or haloperidol (2 mg/kg, 0.2 mg/kg) one week before and one week after the prolonged drug treatment.

Statistical analysis

Data were analyzed using the SPSS computer program (SPSS 19.0 for Windows, Chicago, Illinois, USA). The statistical significance between catalepsy scores was compared by using non-parametric statistical analysis. The Mann-Whitney U Test was used to test for the differences between the treatments on catalepsy score of LEK-8829 *vs.* haloperidol on the first day. The Wilcoxon Signed Rank Test was used to test for the differences between the effects of treatments on catalepsy score on the first *vs.* the last day of the treatment. To evaluate if there was a significant difference between treatment groups in regard the effects of acute treatments on the distance moved parameter, we performed one-way ANOVA followed with Scheffe's multiple comparison test, separately for the test performed before and after the 21 day treatment period, respectively. A paired Student *t*-test was used for the analysis of statistical significances between treatments on distance moved parameter before and after the 21 day treatment. Statistical significance was set at $p < 0.05$ for all statistical analyses.

Results

Catalepsy (experiment 1)

Mann-Whitney U Test revealed no significant difference between the catalepsy scores induced by LEK-8829 2mg/kg and haloperidol 0.2 mg/kg on the first day of the treatment (Fig. 1, - compare A - day 1 *vs.* C - day 1). Wilcoxon Signed Rank Test revealed a statistically significant increase of catalepsy score induced by of 2 mg/kg LEK-8829 on the last day *vs.* the first day of the treatment (Fig. 1, A - compare day 21 *vs.* day 1), but no statistically significant differences between catalepsy scores induced by 2mg/kg of LEK-8829 on the first *vs.* the last day of the treatment (Fig. 1, B - compare day 1 *vs.* day 28) or of the catalepsy scores induced by 2 mg/kg or by 0.2 mg/kg on the firs *vs.* the last day of the treatment (Fig 1, C, D – compare day1 vs. day 21). The treatment with saline or with 0.2 mg/kg of LEK-8829 for 21 did not induce catalepsy (*i.e.* the average catalepsy score during 260 min testing session was below 1) (Fig. 1, D, E).

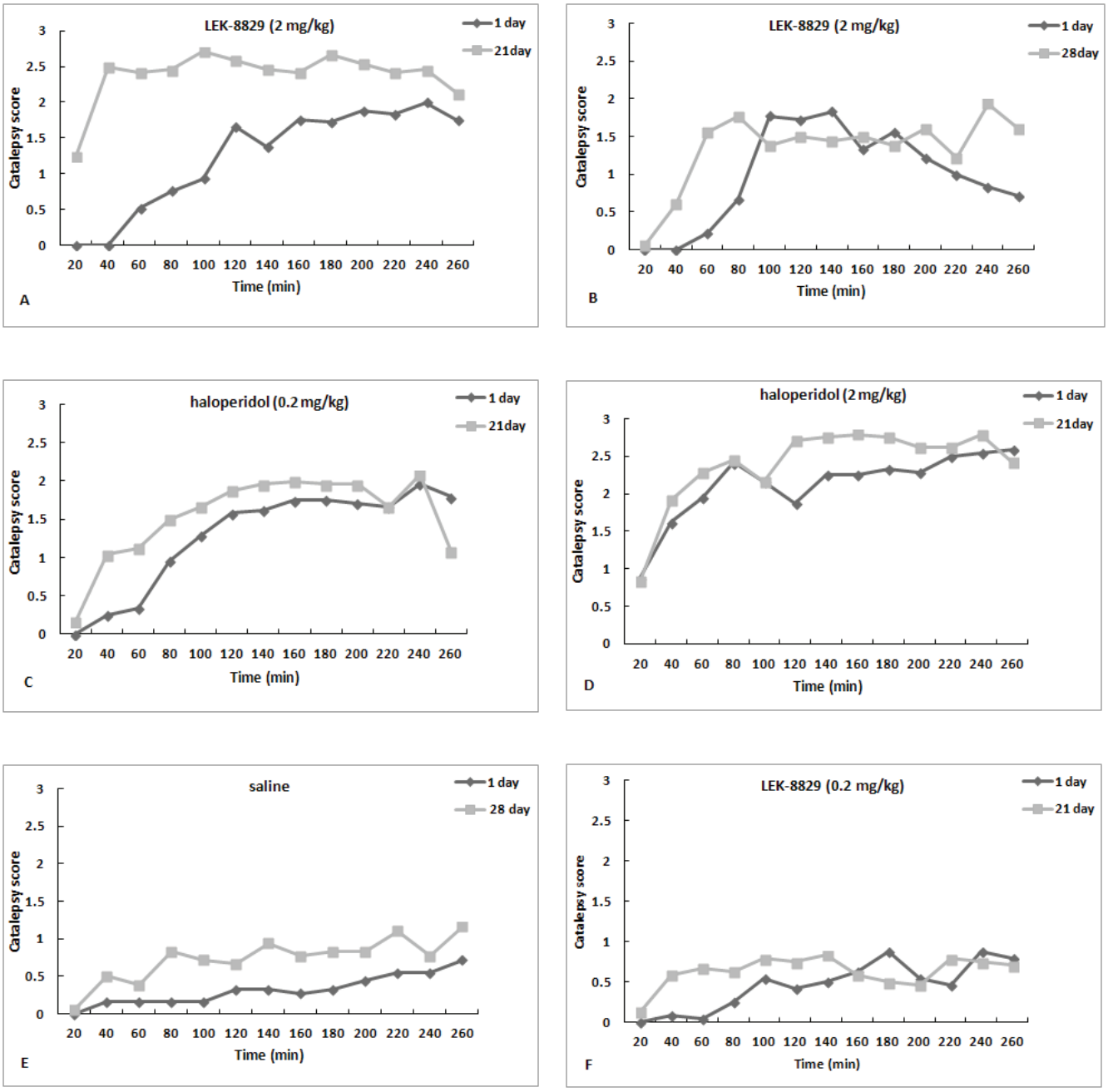

Figure 1: Effect of prolonged treatment with LEK-8829, haloperidol or 0.9% saline on catalepsy

A - LEK-8829 2mg/kg, catalepsy on day 1 and day 21. B - LEK-8829 2mg/kg, catalepsy on day 1 and on day 28. C - haloperidol 0.2 mg/kg group, catalepsy test on day 1 and day 21. D - haloperidol 2 mg/kg group, catalepsy test on day 1 and day 21. E – 0.9 % saline group, catalepsy test on day 1 and day 28. F - LEK-8829 0.2 mg/kg group, catalepsy test on day 1 and on day 21.

Note: on the first treatment (i.e. in drug naïve animals) the dose of 2mg/kg of LEK-8829 was approximately equipotent with the dose of 0.2 mg/kg of haloperidol (compare day 1, **A** and **C**). There was a statistically significant increase of catalepsy in LEK-8829 2mg/kg group on the last day *vs.* the first day of the treatment (compare day 21 *vs.* day 1, **A**) that reverted to previous levels after one week of LEK-8829-free period (compare day 28 *vs.* day 1, **B**). No catalepsy was observed in LEK-8829 0.2 mg/kg group (catalepsy score ≤ 1), (**F**) compare also with absence of catalepsy in 0.9 % saline group (**E**).

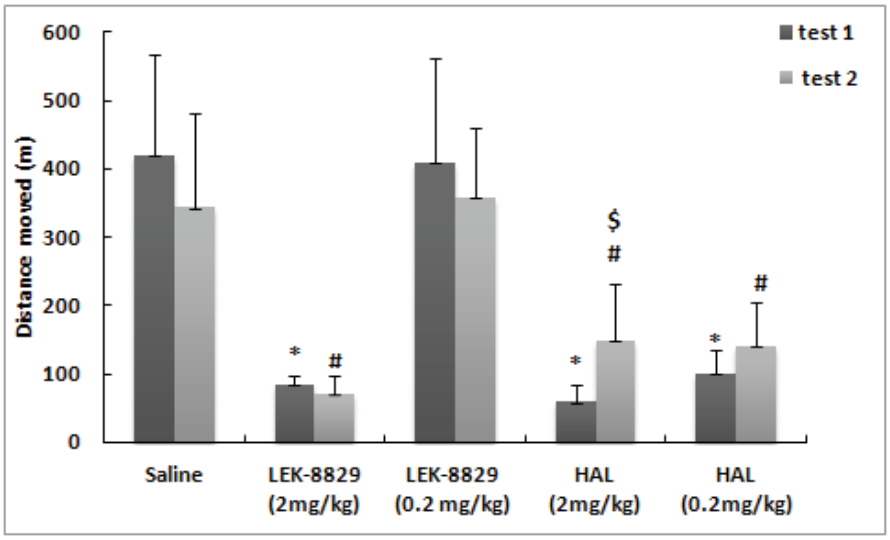

Figure 2: Amhpetamine-induced locomotor activity

* Significant difference as compared with saline group one week before the 21 day treatment period (test 1) with the respective dose of the drug. # Significant difference as compared with saline group one week after the 21 day treatment period (test 2) with the respective dose of drugs (One way ANOVA with Scheffe's post hoc analysis, n = 8, p < 0.05). $ Significant difference as comapred one week before the 21 day treatment vs. one week after the 21 day treatment. (Two-tailed paired Student's t,test).

Inhibition of the amphetamine-induced locomotion (experiment 2)

Both LEK-8829 (2 mg/kg) and haloperidol (2 mg/kg, 0.2 mg/kg) statistically significantly inhibited locomotor activity induced by 2 mg/kg of amphetamine both one week before and one week after the 21 day treatment period with the respective drug (One way ANOVA with Scheffe's post hoc analysis, n = 8, p < 0.05). However, the inhibition of amphetamine-induced locomotor activity after the 21 day treatment by 2 mg/kg of LEK-8829 was equaly effective than the inhibition achieved before the 21 day treatment, while the inhibition by haloperidol after the 21 day treatment by 2 mg/kg haloperidol was significantly less effective than before the 21 day treatment. (Two-tailed paired Student's t, n = 8, p < 0.05). LEK-8829 in the dose of 0.2 mg/kg did not have a significant inhibitory effect when tested neither one week before or one week after the 21 day treatment period and there was also no statistically significant difference between the inhibitory effect of haloperidol in the dose of 0.2 mg/kg one week before and one week after the 21 day treatment period with the respective dose of haloperidol.

Disscusion

In this study we have examined for the first time the effects of prolonged treatment by D2 antagonist/D1 agonist LEK-8829 on its efficacy in behavioral experiments. In preliminary experiments we found that for the induction of catalepsy in drug naive rats the dose of 2 mg/kg of LEK-8829 was approximately equipotent with the dose of 0.2 mg/kg of haloperidol, as scored by behavioral observation during four hours after the injection of the drugs. We have thus assumed that the occupancy of dopamine D2 receptors achieved by these doses of LEK-8829 and haloperidol were approximately equal so that we could then compare the effect of prolonged blockade of dopamine D2 receptors achieved by these doses of LEK-8829 or haloperidol on the efficacy of these two D2 antagonist drugs for the production of catalepsy and for the inhibition of amphetamine-induced locomotor activity.

Catalepsy was proposed to represent an animal model for neuroleptic-induced parkinsonism in humans and it is used as a standard preclinical test to predict antipsychotic activity and motor side-effect liability (17, 23, 24). It is well known that antipsychotics induce catalepsy in rodents (17, 25, 26, 27, 28) and have a dose-dependent propensity to induce EPS in humans and in animals (24). Catalepsy induced by antipsychotics presumably develops due to excessive blockade of dopamine D2 receptors within the basal ganglia. It is characterized by akinesia, the maintenance of even in unusual body posture (9) with waxy rigidity of the limbs, mutism, and complete inactivity, regardless of outside stimuli and may thus be considered to be analogous to sensory neglect, lack of movement and muscle rigidity, such as observed in parkinsonism. A full catalepsy can be induced by blocking either D1 or D2 receptors (17). Coadministration of the D1 and D2 antagonists

has a synergistic effect on catalepsy. However, catalepsy is not a simple motor inactivation due to the blockade of dopaminergic transmission within the basal ganglia, but rather a complex 'active immobility' response (17) that seems to involve more than one neurotransmitter system.

In the first experiment we evaluated the changes in the efficacy of LEK-8829 and of haloperidol for the induction of catalepsy that developed during the prolonged treatment with the respective dose of each drug. We found that only LEK-8829 significantly increased its potential for the induction of catalepsy. Namely, on the last day of the treatment with 2 mg/kg of LEK-8829, the latency for the induction of catalepsy decreased, while the maximal catalepsy score significantly increased and become approximately equipotent with 10X higher dose of haloperidol in drug naive rats (i.e. 2 mg/kg). By comparison, we have speculated that the effect of 21 day treatment with haloperidol on catalepsy might reveal the loss of its efficacy for the induction of catalepsy (26, 29, 30, 31), however, this was also not the case. We speculate that the above results may be explained by the "catalepsy sensitization effect" that develops due to context conditioned learning phenomenon inherent to most of the catalepsy measurement protocols (32, 33). However, when we tested the LEK-8829-treated animals after 7 days of drug-free period, the latency to the onset of catalepsy was decreased, but the catalepsy score reverted to the level induced by 0.2 mg/kg of haloperidol in drug naive animals. We thus speculate that the above results in LEK-8829 treated groups could be better explained by the pharmacokinetic build up and elimination of LEK-8829 in the brain during 21 day treatment period and during the following drug-free period, respectively.

The second experiment showed that in drug naive rats, both LEK-8829 (2 mg/kg) and haloperidol (0.2 mg/kg and 2 mg/kg) almost completely inhibited the locomotor behavior induced by amphetamine (2 mg/kg). However, after the prolonged treatment with the respective drug, only LEK-8829 retained its inhibitory properties, while the inhibition by 2 mg/kg of haloperidol was significantly reduced.

Polonged period of the blockade of dopaminergic transmission induced either by chronic treatment by dopamine D2 antagonist drugs or by the depletion of endogenous dopamine results in the up-regulation of striatal dopamine D2 receptors. The treatment with with most antipsychotic agents thus causes an up-regulation of D2 dopamine receptors, an effect that may result in the loss of their efficacy and the production of irreversible motor side effects such tardive dyskinesia (28, 34). For example, decreases in dopamine receptor input produced by the administration of dopamine receptor antagonists, such as haloperidol, have been shown to increase the levels D2 dopamine receptors (35, 36, 37, 38, 39) and D2 receptor mRNA (40, 41). On the other hand, when selective D2 antagonist is combined with the agonist selective for the D1 receptors, both D2 receptor proliferation and behavioral supersensitivity is completely blocked (29). We therefore speculate that in our experiments the intrinsic activity of LEK-8829 at dopamine D1 receptors may have prevented the up-regulation of dopamine D2 receptors, such as occurs after the prolonged blockade of dopamine D2 receptors with haloperidol. Moreover, prolong periods of dopamine depletion, such as occurs in animal models of parkinsonism could lead to the development of denervational dopaminergic hypersensitivity which is characterized by the functional uncoupling of dopamine receptors, so that when this occurs a selective agonists of either type of dopamine receptors induces psychomotor response, such as locomotor stimulation and stereotypies, even when the experimental animals are simultaneously treated with the antagonist of the opposite type of dopamine receptor. In models of parkinsonism with prolonged dopamine depletion in the brain the intrinsic activity of LEK-8829 at dopamine D1 receptors has been revealed by the robust psychomotor response that seems to be unabated by the concurrent blockade of dopamine D2 receptors by the drug or even by cotreatment with haloperidol (11, 42, 43, 44). We therefore assume, that the decreased efficacy of haloperidol for the inhibition of amphetamine-induced locomotor activity indicates dopamine D2 receptor upregulation that has developed during the period of prolonged treatment with haloperidol, while the prolonged treatment with LEK-8829 did not have such effect. Moreover, our results also imply that the prolonged treatment with LEK-8829 in experimental animals with functioning dopaminergic transmission does not result in the development of the functional uncoupling of dopamine receptors, since by this token the intrinsic activity of LEK-8829 on dopamine D1 receptors would by itself stimulate locomotor

behavior, despite the concomitant blockade of dopamine D2 receptors by the drug.

Conclusions

We conclude that LEK-8829 may retain its antipsychotic efficacy during chronic treatment and that pharmacological profile of atypical antipsychotic drugs with intrinsic activity at dopamine D1 receptors may be beneficial for the prevention of tardive dyskinesia. We therefore speculate that prolonged treatment with LEK-8829 does not result in the up-regulation and/or in the functional uncoupling of dopamine D2 receptors.

References

1. Lewis DA, Lieberman JA. Catching up on schizophrenia: natural history and neurobiology. Neuron. 2000; 28(2): 325–34.

2. Yeganeh-Doost P, Gruber O, Falkai P, Schmitt A. The role of the cerebellum in schizophrenia: from cognition to molecular pathways. Clinics (Sao Paulo). 2011; 66 (Suppl 1): 71–7.

3. Perrault G, Depoortere R, Morel E, Sanger DJ, Scatton B. Psychopharmacological profile of amisulpride: an antipsychotic drug with presynaptic D2/D3 dopamine receptor antagonist activity and limbic selectivity. J Pharmacol Exp Ther 1997; 280(1): 73–82.

4. Wang Y, Xu R, Sasaoka T, Tonegawa S, Kung MP, Sankoorikal EB. Dopamine D2 long receptor-deficient mice display alterations in striatum-dependent functions. J Neurosci 2000; 20(22): 8305–14.

5. Niznik HB, Van Tol HH. Dopamine receptor genes: new tools for molecular psychiatry. J Psychiatry Neurosci 1992; 17(4): 158–80.

6. Tarazi FI, Florijn WJ, Creese I. Differential regulation of dopamine receptors after chronic typical and atypical antipsychotic drug treatment. Neuroscience 1997; 78(4): 985–96.

7. Kapur S, Remington G. Dopamine D(2) receptors and their role in atypical antipsychotic action: still necessary and may even be sufficient. Biol Psychiatry 2001; 50(11): 873–83.

8. Strange PG. Antipsychotic drugs: importance of dopamine receptors for mechanisms of therapeutic actions and side effects. Pharmacol Rev 2001; 53(1): 119–33.

9. Carlsson A, Carlsson ML. A dopaminergic deficit hypothesis of schizophrenia: the path to discovery. Dialogues Clin Neurosci 2006; 8(1):137–42.

10. Meshul CK, Casey DE. Regional, reversible ultrastructural changes in rat brain with chronic neuroleptic treatment. Brain Res 1989; 489(2): 338–46.

11. Hu XT, Wachtel SR, Galloway MP, White FJ. Lesions of the nigrostriatal dopamine projection increase the inhibitory effects of D1 and D2 dopamine agonists on caudate-putamen neurons and relieve D2 receptors from the necessity of D1 receptor stimulation. J Neurosci 1990; 10(7): 2318–29.

12. Krisch I, Bole-Vunduk B, Pepelnak M, et al. Pharmacological studies with two new ergoline derivatives, the potential antipsychotics LEK-8829 and LEK-8841. J Pharmacol Exp Ther 1994; 271(1): 343–52.

13. Zivin M. Potential applications of dopamine D1 agonists and D2 antagonist LEK-8829. Slov Vet Res 2010; 47(4): 175–80.

14. Milivojevic N, Krisch I, Sket D, Zivin M. The dopamine D1 receptor agonist and D2 receptor antagonist LEK-8829 attenuates reinstatement of cocaine-seeking in rats. Naunyn Schmiedebergs Arch Pharmacol 2004; 369(6): 576–82.

15. Jin GZ, Zhu ZT, Fu Y. (-)-Stepholidine: a potential novel antipsychotic drug with dual D1 receptor agonist and D2 receptor antagonist actions. Trends Pharmacol Sci 2002; 23 (1): 4–7

16. Miyagi M, Arai N, Taya F, et al. Effect of cabergoline, a long-acting dopamine D2 agonist, on reserpine-treated rodents. Biol Pharm Bull 1996; 19(11): 1499–502.

17. Frank ST, Schmidt WJ. Burst activity of spiny projection neurons in the striatum encodes superimposed muscle tetani in cataleptic rats. Exp Brain Res 2003; 152(4): 519–22.

18. Wadenberg ML, Soliman A, VanderSpek SC, Kapur S. Dopamine D(2) receptor occupancy is a common mechanism underlying animal models of antipsychotics and their clinical effects. Neuropsychopharmacology 2001; 25(5): 633–41.

19. Reading PJ. Frontal lobe dysfunction in schizophrenia and Parkinson's disease--a meeting point for neurology, psychology and psychiatry: discussion paper. J R Soc Med 1991; 84(6): 349–53.

20. Torres GE. The dopamine transporter proteome. J Neurochem 2006; 97 (Suppl 1): 3–10.

21. Dawe GS, Hwang EH, Tan CH. Pathophy-

siology and animal models of schizophrenia. Ann Acad Med Singapore 2009; 38(5): 425–6.

22. Seeman P. All roads to schizophrenia lead to dopamine supersensitivity and elevated dopamine D2(high) receptors. CNS Neurosci Ther 2011;17(2): 118–32.

23. Xu R, Hranilovic D, Fetsko LA, Bucan M, Wang Y. Dopamine D2S and D2L receptors may differentially contribute to the actions of antipsychotic and psychotic agents in mice. Mol Psychiatry 2002; 7(10): 1075–82.

24. Neve K. The dopamine receptors. 2nd ed. New York: Humana Press, 2010: 441–6.

25. Mandhane SN, Chopde CT, Ghosh AK. Adenosine A2 receptors modulate haloperidol-induced catalepsy in rats. Eur J Pharmacol 1997; 328(2/3): 135–41.

26. Schmidt WJ, Tzschentke TM, Kretschmer BD. State-dependent blockade of haloperidol-induced sensitization of catalepsy by MK-801. Eur J Neurosci 1999; 11(9): 3365–8.

27. Vasconcelos SM, Nascimento VS, Nogueira CR, et al. Effects of haloperidol on rat behavior and density of dopaminergic D2-like receptors. Behav Processes 2003; 63(1): 45–52.

28. Samaha AN, Seeman P, Stewart J, Rajabi H, Kapur S. "Breakthrough" dopamine supersensitivity during ongoing antipsychotic treatment leads to treatment failure over time. J Neurosci 2007; 27(11): 2979–86.

29. Braun AR, Laruelle M, Mouradian MM. Interactions between D1 and D2 dopamine receptor family agonists and antagonists: the effects of chronic exposure on behavior and receptor binding in rats and their clinical implications. J Neural Transm 1997; 104(4/5): 341–62.

30. Barnes DE, Robinson B, Csernanskz JG, Bellows EP. Sensitization versus tolerance to haloperidol-induced catalepsy: multiple determinants. Pharmacol Biochem Behav 1990; 36(4): 883–7.

31. Ezrin-Waters C, Seeman P. Tolerance to haloperidol catalepsy. Eur J Pharmacol 1977; 41 (3):321–7.

32. Banasikowski TJ, Beninеger RJ. Haloperidol conditioned catalepsy in rats: a possible role for D1-like receptors. Int J Neuropsychopharmacol 2012; 15(10): 1525–34.

33. Schmidt WJ, Beninger RJ. Behavioural sensitization in addiction, schizophrenia, Parkinson's disease and dyskinesia. Neurotox Res 2006; 10(2): 161–6.

34. Seeman P. Dopamine receptors and the dopamine hypothesis of schizophrenia. Synapse 1987; 1(2): 133–2.

35. Tarazi FI, Florijn WJ, Creese I. Differential regulation of dopamine receptors after chronic typical and atypical antipsychotic drug treatment. Neuroscience 1997; 78(4):985–96.

36. Laruelle M, Jaskiw GE, Lipska BK, et al. D1 and D2 receptor modulation in rat striatum and nucleus accumbens after subchronic and chronic haloperidol treatment. Brain Res 1992; 575 (1): 47–56.

37. Sirinathsinghji DJ, Schuligoi R, Heavens RP, Dixon A, Iversen SD, Hill RG. Temporal changes in the messenger RNA levels of cellular immediate early genes and neurotransmitter/receptor genes in the rat neostriatum and substantia nigra after acute treatment with eticlopride, a dopamine D2 receptor antagonist. Neuroscience 1994; 62(2): 407–23.

38. Creese I, Burt DR, Snyder SH. Dopamine receptor binding predicts clinical and pharmacological potencies of antischizophrenic drugs. J Neuropsychiatry Clin Neurosci 1996; 8(2): 223–6.

39. Fleminger S, Rupniak NM, Hall MD, Jenner P, Marsden CD. Changes in apomorphine-induced stereotypy as a result of subacute neuroleptic treatment correlates with increased D-2 receptors, but not with increases in D-1 receptors. Biochem Pharmacol 1983; 32(19): 2921–7.

40. Buckland PR, O'Donovan MC, McGuffin P. Both splicing variants of the dopamine D2 receptor mRNA are up-regulated by antipsychotic drugs. Neurosci Lett 1993; 150(1): 25–8.

31. Rouge P, Hanauer A, Zwiller J, Malviya AN, Vincendon G. Up-regulation of dopamine D2 receptor mRNA in rat striatum by chronic neuroleptic treatment. Eur J Pharmacol 1991; 207(2): 165–8.

42. LaHoste GJ, Marshall JF. Dopamine supersensitivity and D1/D2 synergism are unrelated to changes in striatal receptor density. Synapse 1992; 12(1): 14–26.

43. White FJ, Bednarz LM, Wachtel SR, Hjorth S, Brooderson RJ. Is stimulation of both D1 and D2 receptors necessary for the expression of dopamine-mediated behaviors? Pharmacol Biochem Behav 1998;30(1): 189–93.

44. Hu XT, White FJ. Loss of D1/D2 dopamine receptor synergisms following repeated administration of D1 or D2 receptor selective antagonists: electrophysiological and behavioral studies. Synapse 1994; 17(1): 43–61.

UČINKOVITOST POTENCIALNEGA ATIPIČNEGA ANTIPSIHOTIKA LEK-8829 NA VEDENJSKE UČINKE NA PODGANJIH MODELIH KATALEPSIJE TER Z AMFETAMINOM POVZROČENE PSIHOMOTORIČNE STIMULACIJE

S. Bogićević, M. Živin

Povzetek: Antagonisti dopaminskih D2 receptorjev, kot je na primer haloperidol, so učinkovita antipsihotična zdravila, ki pa na žalost pogosto povzročijo neželeni ekstrapiramidni sindrom (EPS).
LEK-8829 je antagonist dopaminskih D2 receptorjev z intrinzično aktivnostjo na dopaminskih receptorjih D1. Predpostavili smo, da intrinzična aktivnost LEK-8829 na dopaminskih receptorjih D1 lahko zmanjša nagnjenost te snovi za povzročanje EPS.
V raziskavi smo preučevali učinke 21 dnevnega tretiranja s haloperidolom oziroma z LEK-8829 na izraženost katalepsije ter na zaviranje z amfetaminom povzročene psihomotorične stimulacije v odprtem polju, tako da smo poskusne podgane vedenjsko testirali pred in po omenjenim 21-dnevnim obdobjem tretiranja in po njem, pri čemer smo uporabili enaka odmerka učinkovin.
Ugotovili smo, da 21 dnevno tretiranje z LEK-8829 oziroma s haloperidolom ni imelo učinka ali pa je celo povečalo njun kataleptični učinek. Po drugi strani pa se je pokazala razlika pri zaviranju z amfetaminom povzročene psihomotorične stimulacije v odprtem polju, pri čemer je bilo zaviranje z LEK-8829 enako učinkovito, zaviranje s haloperidolom pa manj učinkovito kot pri prvem vedenjskem testiranju.
Zato menimo, da bi imel pri zdravljenju shizofrenije potencialni atipični antipsihotik LEK-8829, v primerjavi s tipičnim nevroleptikom haloperidolom, manjšo tendenco za izgubo učinkovitosti ter za povzročanje EPS.

Ključne besede: LEK-8829; dopaminski agonist D1; dopaminski antagonist D2; haloperidol; subkronično tretiranje

Slov Vet Res 2015; 52 (2): 97-102
UDC 636.2.09:636.083.14:615.9:632.958

Case Report

PERACUTE ALPHA-NAPHTHYLTHIOUREA INTOXICATION IN A COW-CALF HERD

Johann Burgstaller[1]*, Kurt Sick[2], Michael-Dieter Mansfeld[2], Romana Steinparzer[3], Thomas Wittek[1]

[1]University Clinic for Ruminants, Department for Farm Animals and Veterinary Public Health, University of Veterinary Medicine Vienna, 1210 Vienna, [2]Carinthian Institute for Veterinary Disease Control, 9020 Klagenfurt, [3]Austrian Agency for Health and Food Safety (AGES), Section Toxicology, 1220 Vienna, Austria

*Corresponding author, E-mail: johann.burgstaller@vetmeduni.ac.at

Summary: This article describes the intoxication of a cow-calf herd (100 animals) with alpha-naphthylthiourea (ANTU), resulting in 10 deaths. The rodenticide, which is not licensed for use in the European Union, might have been introduced into the herd via imported hay or given to the animals maliciously.

Most of the intoxicated animals presented with a peracute condition and sudden death. Clinical signs observed in affected animals included anorexia, rumen stasis, foamy discharge from mouth and nostrils, dyspnea, crackling lung sounds, and abdominal tympanic sounds during acoustic percussion and tachypnea with prominent rib movements. The affected animals were treated symptomatically with glucose, metamizole sodium, caffeine, calcium gluconate, magnesium gluconate and medicinal charcoal. In addition, non-pregnant cows were given dexamethasone. Morbidity among the herd was 13% (13/100) and the case fatality rate was 76.9% (10/13). Post-mortem examination of all cattle carcasses determined cyanotic mucous membranes, serosanguineous liquid containing gelatinous particles in the thoracic cavity and severe lung edema. Histological investigations of lung tissue samples determined a severe and fibrin-rich alveolar and interstitial edema, a mild alveolar histiocytosis and a discrete emigration of granulocytes into alveolar lumens in few locations.

A diagnosis of ANTU intoxication was made. The rodenticide was detected in tissue samples by thin layer chromatography.

To our knowledge, this is the first description of ANTU poisoning within a cattle herd. Since ANTU is still a commonly used rodenticide in many countries, ANTU intoxication should be considered in herds where a substantial number of cattle present with a progressive peracute disease with clinical signs of a white foamy discharge from the mouth and nose, tachypnea and lung edema, leading to high mortality rates.

Key words: ANTU; cattle; edema; feed; intoxication

Introduction

Alpha-naphthylthiourea (ANTU) is a colourless, odourless, crystalline powder used as an active substance in rodenticides. Synonyms include alpha-naphthyl thiocarbamide, 1-naphthyl-thiourea and N (1-naphthyl)-2 thiourea (1). ANTU was discovered by Curt Richter during World War II at the John Hopkins Hospital in Baltimore, United States (2, 3). ANTU is effective against Norway rats whereas house mice and roof rats are increasingly resistant to the compound (3). With respect to the acute toxicity of ANTU among other animal species, pet albino rats and dogs are more susceptible than cats, followed by rabbits (4). Lethal doses differ widely between species, varying from 3 mg/kg for rats, 10 mg/kg for dogs, 25 mg/kg for pigs, 30 mg/kg for horses, 50 mg/kg for cows and 75 mg/kg for cats (1, 5). ANTU

Received: 24 June 2014
Accepted for publication: 4 February 2015

is a neurotoxin which stimulates the sympathetic nervous system and causes substantial leakage of lung capillaries. The consequences of this are pleural effusion, pulmonary edema and respiratory failure (1). According to European regulation (EC) No. 1272/2008 (6), ANTU must be labelled as "fatal if swallowed" and "suspected of causing cancer" if sold within the European Union because of its highly toxic properties. Currently no specific antidote is known. Treatment is supportive and symptomatic (1).

Intoxications of cattle with ANTU may occur due to the use of the rodenticide in barns or during feed production. ANTU can be orally ingested by cattle from their environment or in the feed. However, in the European Union, ANTU is not licensed as an active substance for biocides according to EU directive 98/8/EG (7) and regulation (EU) Nr. 528/2012 (8) or for pesticides according to EU directive 91/414/EWG (9) and regulation (EG) Nr. 1107/2009 (10). This paper describes ANTU intoxication of cows from a cow-calf herd consisting of 50 Simmental cows and their Simmental Charolais crossbreed calves.

Material and methods

Case History

Animals included in this case report originated from a cow-calf herd from Carinthia in the southern part of the Austrian Alps. In addition to the cow-calf operation, the farm also had a separate barn with 80 Simmental and crossbreed finishing cattle.

The cow-calf herd was reared in a free-stall system with access to pasture, while the finishing animals were kept inside permanently. The feed ration of the finishing animals consisted of corn silage, grass silage and concentrate. The cow-calf herd was fed hay only. Drinking water for the livestock was provided by two separate wells.

The first reported incident of ANTU intoxication occurred when the farmer fed hay originating from Italy to the finishing animals (in addition to their usual silage) at the end of December 2011. Since they did not consume the hay in large amounts, he decided to feed it to the cows. The following day four cows were found dead. The imported hay was removed immediately and the carcasses were referred for post-mortem examination to the Carinthian Institute for Veterinary Disease Control.

The second incident occurred when the farmer attempted to feed the imported hay to the finishing group again 2 weeks later. As they did not eat it, he again transferred it over to the cow-calf herd. Over the following four days, 5 cows and 1 bull calf from the cow-calf herd died peracutely. Furthermore, over the course of the two incidents, 2 cases of abortion and 3 cases of retained placenta were noted. All cows and calves in the cow-calf herd were reared in the same barn, so all were exposed to the same feedstuffs. It is reasonable to assume that only the worst affected animals were presented to the veterinarian. Other animals may also have been affected, but recovered without treatment.

Clinical findings

During the first incident, 7 animals were affected and 4 of these died peracutely. The remaining 3 cows suffered from severe clinical signs of intoxication, leading to consultation with the farm veterinarian. The cows appeared lethargic, feed and water intake was decreased and rumen stasis was diagnosed. Skin turgor was slightly decreased, the mucous membranes were slightly cyanotic and scleral congestion was present. The animals were dyspneic with foamy discharge from the mouth and nostrils. The body temperature was within the reference range, while heart rate was increased. Auscultation of the lungs revealed crackling sounds and percussion of the lung fields showed hyperresonance with a tympanic sound. The clinical signs observed in affected animals were compatible with intoxication. In the second incident, 6 animals were affected, all died peracutely, no additional severely affected animals were noted. Overall, smaller cows were more likely to be affected compared to larger, more dominant animals.

Medical treatment

The three cows initially presenting with severe clinical signs of intoxication were treated with an intravenous infusion of 40 % glucose (0.5 l per cow) (Glucosteril 40 %, Fresenius Kabi, Bad Homburg, Germany) and intravenous administration of a veterinary preparation

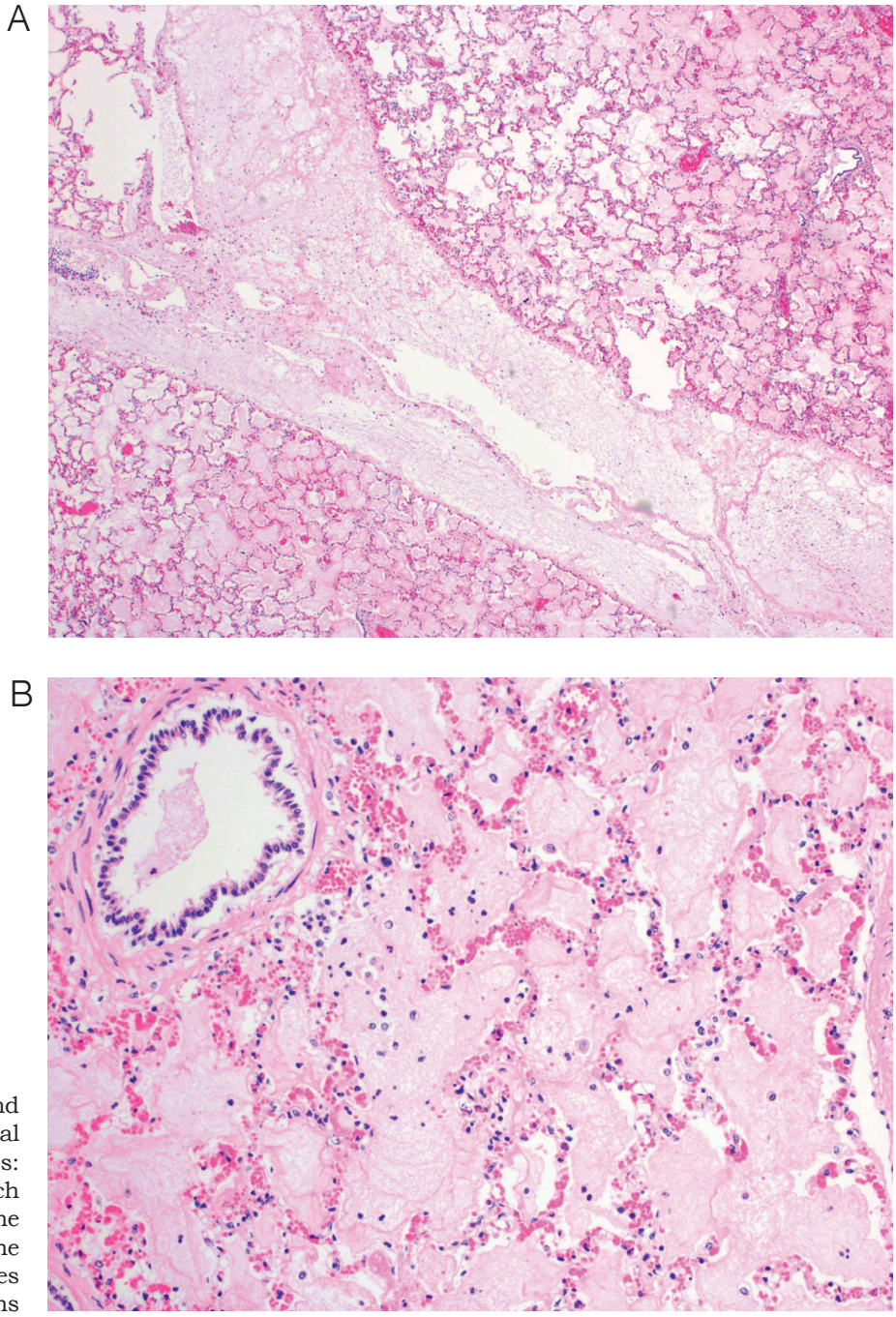

Figure 1: a (magnification x 40) and b (magnification x 400): Histological investigations of lung tissue samples: notice the severe and fibrin-rich alveolar and interstitial edema, the mild alveolar histiocytosis and the discrete emigration of granulocytes into alveolar lumens in some locations

containing metamizole sodium, caffeine, calcium gluconate and magnesium gluconate (0.25 l per cow) (Novacoc forte, Richter Pharma, Wels, Austria). Furthermore, medicinal charcoal was given orally (300 g per animal per day) (Carbopulbit, Bayer, Vienna, Austria). Additionally, non-pregnant cows were treated with an intramuscular injection of dexamethasone (0.06 mg/kg body weight) (Rapidexon, Eurovet Animal Health, Bladel, The Nederlands).

Results

Post-mortem findings

Post-mortem examination of all deceased animals was conducted at the Carinthia Institute for Veterinary Disease Control. Post-mortem examination revealed moderate cyanotic mucous membranes and thoracic cavities filled with a serosanguineous liquid containing gelatinous

particles. The lungs were severely congested and of a brownish-red color. Severe lung edema was noted and gelatinous liquor covered the lungs and extended into the interstitial tissue. Histological examination of the lungs determined severe alveolar and interstitial edema and fibrin-filled alveoli. There were remarkably few inflammatory cells present. (Figure 1a and 1b)

Laboratory investigations

Bacteriological examination failed to isolate any of the major expected pathogens such as Salmonella spp., Campylobacter spp., Pasteurella spp., Mannheimia spp. by culture or Mycoplasma spp., Mycoplasma bovis and mycoides by polymerase chain reaction (PCR). Antigen ELISA also failed to demonstrate the presence of a number of viral pathogens namely: bovine herpes virus type1, bovine virus diarrhea virus, bovine respiratory syncytial virus and bovine parainfluenza virus type 3.

Detection of ANTU in tissue samples

Liver and lung tissue from affected animals was referred to the Institute of Pharmacology, Toxicology and Pharmacy, Ludwig-Maximilians-University Munich, Germany. A thin layer chromatography revealed ANTU residues in the liver tissue (11).

Botanical and toxicological analysis of the feed

A representative sample of the imported hay from Italy was taken by the Official Federal Veterinarian and sent to the Institute of Animal Nutrition and Functional Plant Compounds, Veterinary University of Vienna, Austria. Moderate feeding quality of the hay with impeccable hygiene status was analysed. The hay sample consisted of wild oat (*Avena fatua)*, wildrye (*Elymus sp.)*, vetch (*Lathyrus sp.*), dock (*Rumex sp.*) and dog rose (*Rosa canina)*. Toxic plants were not present. Another sample of the hay was refered to the Austrian Agency for Health and Food Safety (AGES), Department of Animal Nutrition and Feedstuff to analyse the hay for tryptophan residues. Tryptophan was only determined in negligible quantity (0.0807 +/- 0.00807 mass %) by high pressure liquid chromatography (HPLC) according to regulation (EC) No. 152/2009 (12). ANTU could not be detected in hay samples.

Corn crop silage, which was fed to the youngstock on the farm, was analyzed for the occurrence of mycotoxins. Aflatoxin B1, B2, G1, G2 and dexoxynivalenol could not be detected by high pressure liquid chromatography with post-column fluorescence derivatization (HPLC-FLD) and high pressure liquid chromatography with ultra-violet detector (HPLC-UV) respectively.

Discussion

This case report describes intoxication with the rodenticide ANTU among animals from a cow-calf herd in Austria. To our knowledge, ANTU intoxication of a cattle herd has not been described previously.

The clinical features included a peracute progression, respiratory symptoms, foamy discharge from nostrils and mouth and cyanotic mucous membranes in affected animals. The mortality rate of 10 % and case fatality rate of 76.9 % demonstrate the devastating effects on the cow-calf herd. However, the exact number of poisoned animals is unknown since only the worst affected were presented to the veterinarian for examination and treatment. Post-mortem examination determined severely affected lungs, which were congested and edematous. The thoracic cavity was filled with serosanguinous fluid mixed with gelatinous particles. Numerous infectious diseases could be excluded by laboratory examinations as being the possible source of these clinical signs and level of mortality.

ANTU was identified in lung and liver samples from all examined carcasses. How the animals came into contact with the rodenticide is unclear. There may be a link to the imported hay from Italy because the farmer transferred this feed from the finishing unit to the cow-calf herd twice and on both occasions cows died the next day. Although the hay was first fed to the finishing herd, they did not consume it, perhaps due to the additionally provided corn and grass silage in their ration. As the cows in the cow-calf herd were fed solely hay, they had no choice but to eat this feedstuff, regardless of palatability and quality.

To confirm the suspicion of ANTU intoxication, samples of the imported hay were taken by the Official Federal Veterinarian and tested for residues of the rodenticide, however all samples

were negative. One possible reason for these negative results may be the timeframe between the intoxication of the cow-calf herd and the analysis of the hay four months later. Degradation of ANTU during this time could be possible. The feeding of the imported hay was prohibited by the Austrian Authorities for twelve months. After that time the farmer fed the hay to the animals without any ill effect.

Water is a common source of ruminant poisoning (13), and this was provided by two inaccessible wells on farm. There was no overt evidence that the rodenticide was introduced via the water supply, but as unused water drained off continuously this was not tested at the time of the intoxication incidents. The drinking water well was inspected by the local authorities.

Differential diagnoses considered included intoxication of the cow-calf herd with toxic plants. Brassica species, for example, contain glucosinolates which may cause similar clinical signs when fed in high quantities (14). However, no such plants could be identified in the hay fed to the herd. The cow-calf herd had access to the pasture, however, there is no vegetation growth in this region in December and January, therefore feed intake from grassland can be excluded as a possible source of toxin ingestion. Fog fever, caused by an excessive intake of D, L-tryptophan, could also be ruled out because of the very low amounts in the examined hay and the fact that the incident occurred during the winter, as acute bovine pulmonary emphysema and edema (ABPEE) is known to occur when cattle are moved from dry to lush pastures in late summer (14).

It is possible that the cow-calf herd could have ingested ANTU from their environment but, according to the farmer, ANTU was not used on the farm as a rodenticide. This finding was expected, as ANTU use is prohibited throughout the European Union, nevertheless it cannot be excluded that ANTU was given to the animals intentionally.

To conclude, this case report demonstrates evidence of ANTU poisoning among beef cattle as evidenced by rodenticide residues determined in tissue samples upon post-mortem examination. Despite extensive investigations into feed, the farm environment and management factors, the source of the intoxication remains unclear.

Acknowledgements

The authors would like to thank Georg Troyer for clinical advice as veterinarian on the farm and Clair Firth, MVM, for English language assistance.

References

1. Gupta RC. Non-anticoagulant rodenticides. In: Gupta RC, ed. Veterinary toxicology basic and clinical principles. 2nd edition. New York : Academic Press, 2012: 706–7.

2. Richter CP. The development and use of alpha-napthyl thiourea (ANTU) as a rat poison. J Am Med Assoc 1945; 129: 927–31.

3. Gratz N. A critical review of currently used single-dose rodenticides. Bull WHO 1973; 48: 469–77.

4. McClosky WMT, Smith MI. Studies on the pharmacologic action and the pathology of alphanaphtylthiourea (ANTU). Publ Health Rep 1945; 60 (38): 1101–13.

5. Peoples SA. The pharmacology of rodenticides. In: Proceedings of the 4th Vertebrate Pest Conference. Lincoln: University of Nebraska, 1970: 15–8.

6. Anonymous. Regulation (EC) No 1272/2008 of the European Parliament and of the Council of 16 December 2008 on classification, labelling and packaging of substances and mixtures, amending and repealing Directives 67/548/EEC and 1999/45/EC, and amending Regulation (EC) No 1907/2006. Off J EU 2008; L 353: 1–1355 (31. 12. 2008)

7. Anonymous. Directive 98/8/EC of the European Parliament and of the Council of 16 February 1998 concerning the placing of biocidal products on the market. Off J 1998; L 123: 1–63. (24. 4. 1998)

8. Anonymous. Regulation (EU) No 528/2012 of the European Parliament and of the Council of 22 May 2012 concerning the making available on the market and use of biocidal products. Off J EU 2012; L 167: 1–123. (27. 6. 2012)

9. Anonymous. Council Directive of 15 July 1991 concerning the placing of plant protection products on the market (91/414/EEC). Off J EU OJ 1991; L 230: 1–32. (19. 8. 1991)

10. Anonymous. Regulation (EC) No 1107/2009 of the European Parliament and of the Council of 21 October 2009 concerning the placing of plant

protection products on the market and repealing Council Directives 79/117/EEC and 91/414/EEC. Off J EU 2009; L 309: 1–50. (24. 11. 2009)

11. Piskac A, Fejtova I. Detection of rodenticidal preparations - urea derivatives (Dirax, Vacor) in biological materials using thin layer chromatography. Vet Med 1980; 25: 739–42.

12. Anonymous. Commission Regulation (EC) No 152/2009 of 27 January 2009 laying down the methods of sampling and analysis for the official control of feed

13. Ensley S, Rumbeiha W. Ruminant toxicology diagnostics. Vet Clin North Am Food Anim Pract 2012: 28(3): 557–64.

14. Radostits OM, Gay CC, Hinchcliff KW, Constable PD. Diseases of the lungs of cattle in which the essential lesion is interstitial pneumonia. In: Radostits OM, Gay CC, Hinchcliff KW, Constable PD, eds. Veterinary medicine: a textbook of the diseases of cattle, horses, sheep, pigs, and goats. Philadelphia : Saunders Elsevier, 2007: 1998–2003.

PERAKUTNA ZASTRUPITEV Z ALFA-NAFTILTIOUREO V ČREDI KRAV DOJILJ

J. Burgstaller, K. Sick, M. D. Mansfeld, R. Steinparzer, T. Wittek

Povzetek: Ta članek opisuje zastrupitev z alfa-naftiltioureo v čredi krav dojilj (100 živali), ki povzročila 10 smrtnih primerov. Rodenticid, ki sicer ni licenciran za uporabo v Evropski uniji, je bi v čredo vnesen z uvoženim senom ali pa zlonamerno. Pri večini zastrupljenih živali smo opazili perakutno stanje in nenadno smrt. Klinični znaki pri prizadetih živalih so bili naslednji: anoreksija, zastoj vampa, penast izcedek iz ust in nosu, dispneja in prasketajoč zvok v pljučih. Pri perkusiji trebuha smo opazili značilen timpanični zvok in tahipnejo s tipičnim gibanjem reber. Prizadete živali smo simptomatsko zdravili z glukozo, metamizol natrijem, kofeinom, kalcijevim in magnezijevim glukonatom ter medicinskim ogljem. Krave, ki niso bile breje, smo tretirali tudi z deksametazonom. 13% živali v čredi je zbolelo (13/100) in med temi je bila smrtnost 76,9% (10/13). S posmrtnim patološkim pregledom goved smo ugotovili, da so bile sluznice cianotične, v prsni votlini je bila prisotna želatinasta tekočina in hud pljučni edem. S histološko preiskavo vzorcev tkiva pljuč smo ugotovili hud in s fibrinom bogat alveolski in intersticijski edem, blago alveolarno histiocitozo in kar na nekaj mestih diskretno migracijo granulocitov v alveolarni lumen. Naredili smo test na prisotnost ANTU in s tankoplastno kromatografijo odkrili rodenticid v vzorcih tkiva. Po našem mnenju je to prvi opis zastrupitve z rodenticidom ANTU pri govedu. Ker se v mnogih državah ANTU še vedno pogosto uporablja, je potrebno na tovrstno zastupitev v čredah goved pomisliti, če opazimo veliko nenadnih obolenj s kliničnimi znaki, kot je penasti izcedek iz ust in nosu, tahipneja in pljučni edem, ki pripeljejo do visoke stopnje umrljivosti.

Ključne besede: ANTU; govedo; edem; krma; zastrupitev

Namen ustanovitve in delovanja podjetja MD svetovanje d.o.o. je pomagati podjetjem pri poslovanju z nudenjem produktov in storitev, ki ne spadajo v osnovno dejavnost podjetja. To dosegamo s celovito ponudbo predstavljenih produktov in storitev.

Zato smo naš moto Skupaj bomo uspešnejši! nadgradili še z motom in sloganom Vse za Vas na enem mestu!

Vizija

Postati vodilna neodvisna družba s celotno ponudbo za podjetja in posameznike na enem mestu in na ta način prihraniti podjetjem in posameznikom čas in denar.

Vse to nam bo uspelo s trdim delom in kakovostno izvedbo storitev in zaupanih nam nalog, predvsem če bomo sledili naslednjim načelom:

- zagotavljanje celovite ponudbe,
- vedno delo v dobro stranke,
- strokoven razvoj,
- organizacijsko izpopolnjevanje,
- zagotavljanje visoke stopnje kakovosti storitev z upoštevanjem predlogov naših strank,
- ustvarjanje novih delovnih mest,
- povečanje produktivnosti in dobičkonosnosti,
- visoko motiviran in usposobljen kader s primernim vodenjem, kar zagotavlja
- kakovost izvajanja storitev,
- postati vodilno podjetje, ki ponuja rešitve, ki podjetju omogočajo da si na enem
- mestu zagotovi vse dejavnosti, ki ne spadajo v njegovo osnovno dejavnost.

Prednosti poslovanja z nami:

- vse svoje potrebe in vizije uresničite s klicem na eno telefonsko številko,
- razbremenite se ukvarjanja z obrobnimi zadevami,
- posvetite se svojemu strokovnemu delu,
- informacijska tehnologija,
- prilagodljivost,
- zanesljivost,
- povečanje dobičkonosnosti,
- zmanjšanje stroškov dela,
- ...

MD svetovanje, poizvedbe in storitve d.o.o.
Dunajska cesta 421,
1231 Ljubljana – Črnuče

PE Ljubljana-Vič
Cesta dveh cesarjev 403,
1102 Ljubljana

01 / 620-47-01
01 / 620-47-04
041 / 614-090

www. mdsvetovanje. eu

Zakaj MD Svetovanje d.o.o.

- visoka profesionalizacija,
- visoka strokovnost,
- visoka uspešnost,
- konkurenčne cene,
- vse na enem mestu.

mdinfo@mdsvetovanje.eu www.mdsvetovanje.eu

SLOVENIAN VETERINARY RESEARCH
SLOVENSKI VETERINARSKI ZBORNIK

Slov Vet Res 2015; 52 (2)

Original Scientific Articles

Špehar M, Mrak V, Smetko A, Potočnik K, Gorjanc G. Genome-wide association study for dairy traits in Slovenian Brown Swiss breed 49
Jaćimović M, Lenhardt M, Višnjić-Jeftić Ž, Jarić I, Gačić Z, Hegediš A, Krpo-Ćetković J. Elemental concentrations in different tissues of European perch and black bullhead from Sava Lake (Serbia) 57
Smodiš Škerl MI, Gregorc A. Characteristics of hypopharyngeal glands in honeybees (*Apis mellifera carnica*) from a nurse colony 67
Krek JL, Šimundić M, Drab M, Pajnič M, Šuštar V, Štukelj R, Drobne D, Veronika Kralj-Iglič V. Effect of carbon black nanomaterial on canine erythrocyte and platelet shape 75
Bogićević S, Živin M. Efficacy of potential atypical antipsychotic lek-8829 on behavioral effects in rat model of catalepsy and inhibition of amphetamine induced psychomotor stimulation..... 87

Case Report

Burgstaller J , Sick K, Mansfeld MD, Steinparzer R, Wittek T. Peracute alpha-naphthylthiourea intoxication in a cow-calf herd ... 97